Topology-preserving rigid transformation of 2D digital images

Phuc Ngo, Nicolas Passat, Yukiko Kenmochi, Hugues Talbot

Topology-preserving rigid transformation of 2D digital images

Phuc Ngo, Nicolas Passat, Yukiko Kenmochi, Hugues Talbot

***Abstract*—We provide conditions under which 2D digital images preserve their topological properties under rigid transformations. We consider the two most common digital topology models, namely dual adjacency and well-composedness. This study leads to the proposal of optimal preprocessing strategies that ensure the topological invariance of images under arbitrary rigid transformations. These results and methods are proved to be valid for various kinds of images (binary, grey-level, label), thus providing generic and efficient tools, that can be used in particular in the context of image registration and warping.**

***Index Terms*—Digital images, rigid transformation, digital topology, image preprocessing, registration, warping.**

I. Introduction

In image computing, the preservation of topological properties is a crucial issue. Indeed, topological properties provide useful information and descriptors when performing image processing and analysis tasks such as segmentation [1], classification [2], registration [3] or tracking [4]. This concerns not only 3D (*e.g.*, in medical imaging [5]) but also 2D data (*e.g.*, in remote sensing [6] or computer vision [7]). In particular, topology preservation – pioneered nearly fifty years ago [8], [9] – has been investigated in the context of image transformation, both from the viewpoints of registration [10] and warping [11]. To this end, efforts have been mainly devoted to handling complex transformations, while simpler ones have remained largely under-considered.

The handling of such transformations (*e.g.*, translations, rotations) is often assumed to be almost trivial. Indeed, in $\mathbb{R}^n$, most are topology-preserving, while this is not necessarily the case for complex ones (induced, *e.g.*, by nonrigid registration [12]). Based on this assertion, it is often assumed that simple transformations also lead to trouble-free handling of topological properties in $\mathbb{Z}^n$. This is a wrong belief.

In the case of rigid transformations in $\mathbb{Z}^2$ [13], which include the family of rotations [14], [15], [16], [17], [18], some topological issues have been identified [19], [20]. They are induced by the sampling operation, which is mandatory to guarantee the stability of the transformations inside $\mathbb{Z}^2$.

In this article, that is an extended and improved version of the conference paper [21], we deal with these topological issues (Sec. III), and we provide some methods for topological analysis and preprocessing of images before rigid transformations. We first give some conditions under which a 2D digital image preserves its topological properties under arbitrary rigid transformations (Sec. IV). Then, we propose methods for analysing and preprocessing digital images before rigid transformation, in order to preserve their topological properties (Sec. V). This study is generic on two sides: (i) the main two digital topology models are considered, namely the dual adjacency, and the well-composedness ones; and (ii) the cases of binary, grey-level and label images are dealt with. Experiments are finally proposed (Sec. VI). The article is concluded by perspective works (Sec. VII). For the sake of readability, technical proofs are reported in Appendix A.

Phuc Ngo, Yukiko Kenmochi and Hugues Talbot are with the ESIEE-Paris and the Université Paris-Est, LIGM UMR CNRS 8049, Paris, France ({h.ngo,y.kenmochi,h.talbot}@esiee.fr).

Nicolas Passat is with the Université de Reims Champagne-Ardenne, CReSTIC EA 3804, Reims, France (nicolas.passat@univ-reims.fr).

II. Background notions

A. Notations

The sets are noted $\mathbb{A}$, $\mathbb{B}$, $\mathbb{C}$, *etc*., and their subsets are noted A, B, Γ, *etc*. The power set of a set A is noted 2^{A}. The elements of sets are noted a, b, c, *etc*., and $\mathbf{a}$, $\mathbf{b}$, $\mathbf{c}$, *etc*. if the set is a Cartesian product. By abuse of notation, an element that should be noted as a column vector $\binom{a}{b}$ is noted as a line vector (a, b).

The functions defined on continuous sets are noted $\mathcal{A}$, $\mathcal{B}$, $\mathcal{C}$, *etc*., and the ones defined on discrete sets are noted A, B, C, *etc*. A function F from $\mathbb{A}$ to $\mathbb{B}$ is noted $F : \mathbb{A} \to \mathbb{B}$. If $\mathrm{A} \subseteq \mathbb{A}$ and $\mathrm{B} \subseteq \mathbb{B}$, we note $F(\mathrm{A}) = \{F(x) \mid x \in \mathrm{A}\}$ and $F^{-1}(\mathrm{B}) = \{x \mid F(x) \in \mathrm{B}\}$. If F is a bijection, its inverse function is also noted $F^{-1} : \mathbb{B} \to \mathbb{A}$. The restriction of $F : \mathbb{A} \to \mathbb{B}$ to the subset $\mathrm{A} \subseteq \mathbb{A}$ is noted $F_{|\mathrm{A}} : \mathrm{A} \to \mathbb{B}$. The composition of $F : \mathbb{A} \to \mathbb{B}$ and $G : \mathbb{B} \to \mathbb{C}$ is noted $G \circ F : \mathbb{A} \to \mathbb{C}$. The spaces of functions are noted $\mathcal{A}$, $\mathcal{B}$, $\mathcal{C}$, *etc*.

Adjacency (*i.e.*, binary, irreflexive and symmetric) relations are noted $\frown$. Equivalence (*i.e.*, binary, reflexive, transitive and symmetric) relations are noted $\sim$. We recall that a relation $\frown$ (resp. $\sim$) defined on a set A is actually a subset of A×A, and that $a \frown b$ (resp. $a \sim b$) means that $(a, b) \in \frown$ (resp. $\sim$). Given a set A, equipped with an equivalence relation $\sim$, the equivalence class of $a \in \mathrm{A}$ with respect to $\sim$ is noted $[a]_{\sim}$, and the quotient set of A with respect to $\sim$ is noted $\mathrm{A}/\!\sim$.

The most important notations further introduced are recalled in Table I.

B. Rigid transformations

1) Continuous case: In $\mathbb{R}^2$, a rigid transformation is a function

$$\left| \begin{array}{rcccc} \mathcal{U} & : & \mathbb{R}^2 & \to & \mathbb{R}^2 \\ & & \mathbf{x} & \mapsto & \mathbf{R}.\mathbf{x} + \mathbf{t} \end{array} \right. \tag{1}$$

where $\mathbf{R}$ is a rotation matrix, and $\mathbf{t} \in \mathbb{R}^2$ is a translation vector. The function $\mathcal{U}$ is a bijection, and we note $\mathcal{T} = \mathcal{U}^{-1}$

TABLE I
PRINCIPAL NOTATIONS

$\mathcal{C}^\star[I]$	connected components of I
$\mathcal{T}^\star(I)$	adjacency tree of I
$\mathcal{RIG}_{\mathbb{R}^2}$, $\mathcal{RIG}_{\mathbb{Z}^2}$	rigid transformations
$\mathcal{IM}_{\mathbb{B}}$, $\mathcal{IM}_{\mathbb{G}}$, $\mathcal{IM}_{\mathbb{L}}$	finite images
$\mathcal{WC}_{\mathbb{B}}$, $\mathcal{WC}_{\mathbb{G}}$, $\mathcal{WC}_{\mathbb{L}}$	well-composed images
$\mathcal{NS}_{\mathbb{B}}$, $\mathcal{NS}_{\mathbb{G}}$, $\mathcal{NS}_{\mathbb{L}}$	well-composed, non-singular images
$\mathcal{RES}_{\mathbb{B}}$, $\mathcal{RES}_{\mathbb{G}}$, $\mathcal{RES}_{\mathbb{L}}$	regular images
$\mathcal{INV}^\star_{\mathbb{B}}$, $\mathcal{INV}^\star_{\mathbb{G}}$, $\mathcal{INV}^\star_{\mathbb{L}}$	topologically invariant images

its inverse function, which is also a rigid transformation. We note $\mathcal{RIG}_{\mathbb{R}^2}$ the set of all the rigid transformations.

2) Discrete case: These definitions cannot be directly applied when considering $\mathbb{Z}^2$ instead of $\mathbb{R}^2$. Indeed, there is no guarantee that $\mathcal{U}(\mathbb{Z}^2) \subseteq \mathbb{Z}^2$. The handling of *discrete* rigid transformations then requires to consider a discretisation operator $\mathcal{D} : \mathbb{R}^2 \to \mathbb{Z}^2$. Generally, $\mathcal{D}$ is a standard rounding function, *e.g.*, the floor or ceiling functions. We can then define the discrete analogues $U : \mathbb{Z}^2 \to \mathbb{Z}^2$ and $T : \mathbb{Z}^2 \to \mathbb{Z}^2$, of $\mathcal{U}$ and $\mathcal{T}$, as

$$U = \mathcal{D} \circ \mathcal{U}_{|\mathbb{Z}^2} \tag{2}$$

$$T = \mathcal{D} \circ \mathcal{T}_{|\mathbb{Z}^2} = D \circ (\mathcal{U}^{-1})_{|\mathbb{Z}^2} \tag{3}$$

We note $\mathcal{RIG}_{\mathbb{Z}^2}$ the set of all the discrete rigid transformations.

3) Transformation models: Two transformation models can be considered for discrete (rigid) transformations.

The Lagrangian model consists of computing $U(\mathbb{Z}^2)$. From the viewpoint of image computing, this is not suitable, since U is often neither injective nor surjective. In other words, if U is applied on a digital image (Sec. II-C), it may lead to a transformed image that will present both undefined and conflicted values.

The Eulerian model, considered in this work, consists of computing $T(\mathbb{Z}^2)$. From an imaging viewpoint, this is more satisfactory, since T is defined on the whole transformed space $\mathbb{Z}^2$, thus guaranteeing that any point of a transformed digital image will be unambiguously defined. Nevertheless, since T presents the same properties as U in terms of non-injectivity and non-surjectivity, this model is not exempt from topological difficulties.

C. Digital images

We consider *finite* digital images $I : \mathbb{Z}^2 \to \mathbb{V}$. This means that there exists a background value $b \in \mathbb{V}$ such that $I^{-1}(\mathbb{V} \setminus \{b\})$ is of finite extent.

We consider three frequently used value sets $\mathbb{V}$:

- $\mathbb{B} = \{0, 1\}$;
- $\mathbb{G} \subseteq \mathbb{Z}$ or $\mathbb{R}$ (equipped with the canonical order $\leqslant$);
- $\mathbb{L}$, being any arbitrary set (not equipped with any order).

The first case ($\mathbb{V} = \mathbb{B}$) deals with binary images. The set of all finite binary images is noted $\mathcal{IM}_{\mathbb{B}}$. The second case ($\mathbb{V} = \mathbb{G}$) deals with grey-level images. Without loss of generality, we assume that $b = \bigwedge^{\leqslant} \mathbb{G}$. The set of all finite grey-level images is noted $\mathcal{IM}_{\mathbb{G}}$. The third case ($\mathbb{V} = \mathbb{L}$) deals with label images. The set of all finite label images is noted $\mathcal{IM}_{\mathbb{L}}$.

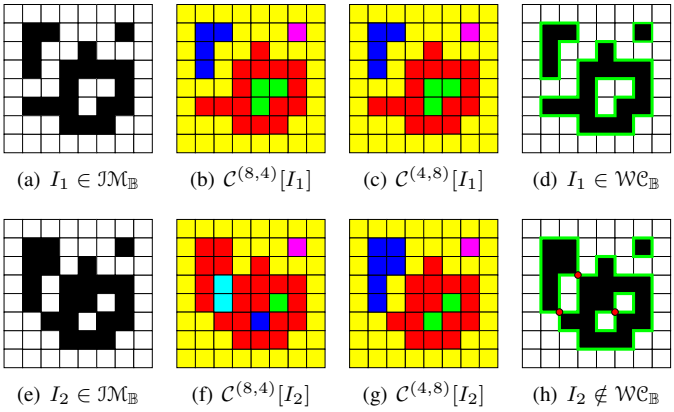

(a) $I_1 \in \mathcal{IM}_{\mathbb{B}}$ (b) $\mathcal{C}^{(8,4)}[I_1]$ (c) $\mathcal{C}^{(4,8)}[I_1]$ (d) $I_1 \in \mathcal{WC}_{\mathbb{B}}$

(e) $I_2 \in \mathcal{IM}_{\mathbb{B}}$ (f) $\mathcal{C}^{(8,4)}[I_2]$ (g) $\mathcal{C}^{(4,8)}[I_2]$ (h) $I_2 \notin \mathcal{WC}_{\mathbb{B}}$

Fig. 1. (a) A binary image $I_1 \in \mathcal{IM}_{\mathbb{B}}$. (b) If we consider I_1 as a $(8,4)$-image, the 8-connected components of $\Omega = I_1^{-1}(\{1\})$ are depicted in blue, purple and red, while the 4-connected components of $\overline{\Omega} = I_1^{-1}(\{0\})$ are depicted in yellow and green. (c) If we consider I_1 as a $(4,8)$-image, the 4-connected components of Ω are depicted in blue, purple and red, while the 8-connected components of $\overline{\Omega}$ are depicted in yellow and green. Note that since I_1 has the same topological structure as a $(8,4)$- and as a $(4,8)$-image, it can also be considered in the well-composedness model: the boundaries shared by its foreground and background regions, depicted in green (d), are 1-manifolds. (e) A binary image $I_2 \in \mathcal{IM}_{\mathbb{B}}$. (f) If we consider I_2 as a $(8,4)$-image, the 8-connected components of $\Omega = I_2^{-1}(\{1\})$ are depicted in purple and red, while the 4-connected components of $\overline{\Omega} = I_2^{-1}(\{0\})$ are depicted in yellow, cyan, blue and green. (g) If we consider I_2 as a $(4,8)$-image, the 4-connected components of $\Omega = I_2^{-1}(\{1\})$ are depicted in blue, purple and red, while the 8-connected components of $\overline{\Omega} = I_2^{-1}(\{0\})$ are depicted in yellow and green. Note that I_2 does not have the same topological structure as a $(8,4)$- and as a $(4,8)$-image. Thus, I_2 is ill-composed: the boundaries shared by its foreground and background regions, depicted in green, are not 1-manifolds (see the red dots in (h)). (a,d,e,h) Ω is depicted in black, and $\overline{\Omega}$ in white. (b,c,f,g) For the sake of readability, each connected component is represented in a different colour.

Remark 1: For the sake of readability, a point $\mathbf{p} = (x, y) \in \mathbb{Z}^2$ will be associated to the *pixel* $[x-\frac{1}{2}, x+\frac{1}{2}] \times [y-\frac{1}{2}, y+\frac{1}{2}] \subset \mathbb{R}^2$. All the figures rely on this digital interpretation.

D. Digital topology

1) Basic notions: Digital topology [22] provides a simple framework for handling the topology of binary images in $\mathbb{Z}^n$. It is also compliant [23] with other discrete models (*e.g.*, Khalimsky grids [24] and cubical complexes [25]) but also with continuous notions of topology [26].

Practically, digital topology relies on two adjacency relations, noted $\frown_{2n}$ and $\frown_{3^n-1}$, defined, for any $\mathbf{p}, \mathbf{q} \in \mathbb{Z}^n$, by

$$\big(\mathbf{p} \frown_{2n} \mathbf{q}\big) \iff \big(\|\mathbf{p} - \mathbf{q}\|_1 = 1\big) \tag{4}$$

$$\big(\mathbf{p} \frown_{3^n-1} \mathbf{q}\big) \iff \big(\|\mathbf{p} - \mathbf{q}\|_\infty = 1\big) \tag{5}$$

In the case of $\mathbb{Z}^2$, we retrieve the well-known 4- and 8-adjacency relations.

Let $\Omega \subseteq \mathbb{Z}^2$. We say that $\mathbf{p}, \mathbf{q} \in \mathbb{Z}^2$ are 4- (resp. 8-) adjacent, if $\mathbf{p} \frown_4 \mathbf{q}$ (resp. $\mathbf{p} \frown_8 \mathbf{q}$). From the reflexive-transitive closure of $\frown_4$ (resp. $\frown_8$) on Ω, we derive the 4- (resp. 8-) connectedness relation $\sim_4$ (resp. $\sim_8$) on Ω; we say that $\mathbf{p}, \mathbf{q}$ are 4- (resp. 8-) connected in Ω, if $\mathbf{p} \sim_4 \mathbf{q}$ (resp. $\mathbf{p} \sim_8 \mathbf{q}$). It is plain that $\sim_4$ (resp. $\sim_8$) is an equivalence relation on Ω; the equivalence classes $\Omega/\sim_4$ (resp. $\Omega/\sim_8$) are called the 4- (resp. 8-) connected components of Ω.

2) Dual adjacency and well-composedness models: A finite set $\Omega \subset \mathbb{Z}^2$ can be modeled as a binary image $I \in \mathcal{IM}_{\mathbb{B}}$, defined by $I^{-1}(\{1\}) = \Omega$ and $I^{-1}(\{0\}) = \overline{\Omega} = \mathbb{Z}^2 \setminus \Omega$, or vice versa. The topological handling of I cannot easily rely on a single adjacency relation for both Ω and $\overline{\Omega}$, due to paradoxes related to the discrete version of the Jordan theorem [27]. Such paradoxes are avoided by considering distinct adjacencies for Ω and $\overline{\Omega}$, leading to the dual adjacency model [28] (Fig. 1(e–g)).

Definition 2 (Dual adjacency [28]): Let $I \in \mathcal{IM}_{\mathbb{B}}$. Let $\Omega = I^{-1}(\{1\})$ and $\overline{\Omega} = I^{-1}(\{0\})$. We say that I is a $(8,4)$- (resp. a $(4,8)$-) *image* if Ω is equipped with $\frown_8$ (resp. $\frown_4$), while $\overline{\Omega}$ is equipped with $\frown_4$ (resp. $\frown_8$). We define the set of the connected components of the $(8,4)$- (resp. $(4,8)$-) image I as

$$\mathcal{C}^{(8,4)}[I] = I^{-1}(\{1\})/{\sim_8} \cup I^{-1}(\{0\})/{\sim_4} \quad (6)$$
$$(\text{resp. } \mathcal{C}^{(4,8)}[I] = I^{-1}(\{1\})/{\sim_4} \cup I^{-1}(\{0\})/{\sim_8})$$

For the sake of concision, we will often write $(k, \overline{k})$ as a unified notation for $(8,4)$ and $(4,8)$.

Alternatively, both Ω and $\overline{\Omega}$ may be equipped with $\frown_4$, provided one considers only images that avoid the issues related to the Jordan theorem, *i.e.*, those for which $\sim_4$ and $\sim_8$ are equivalent for both Ω and $\overline{\Omega}$, thus leading to the well-composedness model [29] (Fig. 1(a–c)).

Definition 3 (Well-composedness [29]): Let $I \in \mathcal{IM}_{\mathbb{B}}$. We say that I is a *well-composed* (or a *wc*-) *image* if

$$\forall v \in \mathbb{B}, I^{-1}(\{v\})/{\sim_8} = I^{-1}(\{v\})/{\sim_4} \quad (7)$$

We define the set of the connected components of the *wc*-image I as

$$\mathcal{C}^{wc}[I] = I^{-1}(\{1\})/{\sim_4} \cup I^{-1}(\{0\})/{\sim_4} \quad (8)$$

The set of the finite well-composed binary images is noted $\mathcal{WC}_{\mathbb{B}}$.

Remark 4: When interpreting digital topology in a continuous framework [23], an image is well-composed iff the boundaries shared by the foreground and background regions are manifolds [29] (Fig. 1(d,h)).

Remark 5: The well-composedness model is more restrictive than dual adjacency. Indeed, any $I \in \mathcal{IM}_{\mathbb{B}}$ can be considered in the dual adjacency model, but not necessarily in the well-composedness one, *i.e.*

$$\mathcal{WC}_{\mathbb{B}} \subset \mathcal{IM}_{\mathbb{B}} \quad (9)$$

III. Purpose

Given an image $I \in \mathcal{IM}_{\mathbb{V}}$, a transformation $T : \mathbb{Z}^2 \to \mathbb{Z}^2$, and the transformed image $I_T \in \mathcal{IM}_{\mathbb{V}}$ obtained from I and T, a frequent question in image analysis is: *"Does T preserve the topology between I and I_T?"*. It is generally answered by observing the topological invariants of these images.

Among the simplest are the Euler-Poincaré characteristic and the Betti numbers. However, these are too weak to accurately model "topology preservation" between images [27]. It is necessary to consider stronger topological invariants, *e.g.*, the (digital) fundamental group [30], the homotopy-type

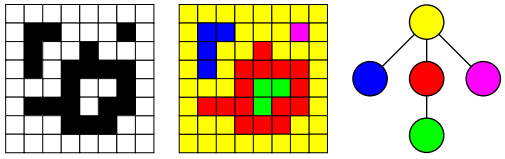

(a) (b) (c)

Fig. 2. (a) The binary image of Fig. 1(a). (b) The connected components of the background (in yellow and green) and foreground (in red, blue and purple) of (a). (c) The adjacency tree associated to (a) in which each coloured node corresponds to a connected component of (a,b), while each edge corresponds to an adjacency link between two components. The root of the tree is the yellow node, that corresponds to the infinite background component in (a,b).

(considered via notions of simple points/sets [31], [32], [33], [34]), or the adjacency tree [35].

Our first goal is to provide conditions under which 2D digital images preserve their topological properties under arbitrary rigid transformations. A crucial issue is the choice of the topological invariant used to formalise this problem. Any of those evoked above describe topology preservation in a *global* fashion, and do not model accurately the possible *local* modifications of the image topological structure. Indeed, I and I_T may have identical fundamental group, homotopy-type and/or adjacency tree while still retaining some topological differences between regions of I and I_T that are in correspondence with respect to T. (A classical example that illustrates this assertion is the "scorpion" configuration illustrated, *e.g.*, in [36], where the removal of a point from a 3D object removes a tunnel while simultaneously creating another, thus producing a new object with the same global topological invariants. However this procedure changes the local topological structure in the neighbourhood of these two tunnels.)

In the sequel, we propose some conditions to achieve this first goal. Our conjecture is that these conditions are *necessary and sufficient* to *locally* preserve image topological properties under arbitrary rigid transformations. However, in this article, we only establish that they are *sufficient* to *globally* preserve image topological properties under any rigid transformation.

Indeed, on the one hand, the proof of the whole conjecture would require the development of a heavy theoretical framework, that falls out of the scope of this journal (Sec. VII). On the other hand, the fact that our proposed conditions are sufficient is the result that is actually useful for image preprocessing. This is the second goal of this article, and probably the most interesting for many readers.

We consider the adjacency tree [35] as a (global) topological invariant. The motivation of this choice is twofold: (i) understanding this topological invariant is probably easier for most readers; and (ii) in the 2D case, its preservation is equivalent [37] to the preservation of the homotopy-type, that is the most commonly used topological invariant in image processing. We now recall the definition of the adjacency tree.

Let $I \in \mathcal{IM}_{\mathbb{B}}$ (resp. $\mathcal{WC}_{\mathbb{B}}$). Let $\Omega_1, \Omega_2 \in \mathcal{C}^{(k,\overline{k})}[I]$ (resp. $\mathcal{C}^{wc}[I]$), with $\Omega_1 \neq \Omega_2$. We note $\Omega_1 \frown_I^{(k,\overline{k})} \Omega_2$ (resp. $\Omega_1 \frown_I^{wc} \Omega_2$) if there exist $\mathbf{p} \in \Omega_1$ and $\mathbf{q} \in \Omega_2$ such that $\mathbf{p} \frown_4 \mathbf{q}$. It is plain that $\frown_I^{(k,\overline{k})}$ (resp. $\frown_I^{wc}$) is an adjacency relation, and that $\Omega_1 \frown_I^{(k,\overline{k})} \Omega_2$ implies that $\Omega_1 \in I^{-1}(\{1\})/{\sim_k}$ and

$\Omega_2 \in I^{-1}(\{0\})/\sim_{\overline{k}}$ or vice versa. We define the $(k,\overline{k})$- (resp. wc-) *adjacency graph* of I as $\mathcal{G}^{(k,\overline{k})}(I) = (\mathcal{C}^{(k,\overline{k})}[I], \frown_I^{(k,\overline{k})})$ (resp. $\mathcal{G}^{wc}(I) = (\mathcal{C}^{wc}[I], \frown_I^{wc})$). This graph is connected and acyclic, and is indeed a tree. It can be equipped with a root that is the (only) infinite connected component of $\mathcal{C}^{(k,\overline{k})}[I]$ (resp. $\mathcal{C}^{wc}[I]$), thus leading to the following definition.

Definition 6 (Adjacency tree [35]): Let $I \in \mathcal{IM}_{\mathbb{B}}$ (resp. $\mathcal{WC}_{\mathbb{B}}$). The $(k,\overline{k})$- (resp. wc-) *adjacency tree* of I is the triplet

$$\mathcal{T}^{(k,\overline{k})}(I) = \left(\mathcal{C}^{(k,\overline{k})}[I], \frown_I^{(k,\overline{k})}, B_I^{(k,\overline{k})}\right) \quad (10)$$
$$\text{(resp. } \mathcal{T}^{wc}(I) = \left(\mathcal{C}^{wc}[I], \frown_I^{wc}, B_I^{wc}\right) \text{)}$$

where $B_I^{(k,\overline{k})} \in \mathcal{C}^{(k,\overline{k})}[I]$ (resp. $B_I^{wc} \in \mathcal{C}^{wc}[I]$) is the unique infinite connected component of I.
An adjacency tree example is given in Fig. 2.

We are now ready to present our definition of topology preservation under rigid transformation.

Definition 7 (Topological invariance): Let $I \in \mathcal{IM}_{\mathbb{B}}$ (resp. $\mathcal{WC}_{\mathbb{B}}$). We say that I is $(k,\overline{k})$- (resp. wc-) *topologically invariant* if $I \circ T \in \mathcal{IM}_{\mathbb{B}}$ (resp. $\mathcal{WC}_{\mathbb{B}}$) and if any $T \in \mathcal{RIG}_{\mathbb{Z}^2}$ induces an isomorphism between $\mathcal{T}^{(k,\overline{k})}(I)$ (resp. $\mathcal{T}^{wc}(I)$) and $\mathcal{T}^{(k,\overline{k})}(I \circ T)$ (resp. $\mathcal{T}^{wc}(I \circ T)$). We note $\mathcal{INV}_{\mathbb{B}}^{(k,\overline{k})}$ (resp. $\mathcal{INV}_{\mathbb{B}}^{wc}$) the set of all the $(k,\overline{k})$- (resp. wc-) topologically invariant binary images.

IV. Theoretical results

In this section, we define a notion of *regularity* (Sec. IV-C) that provides conditions under which binary images are topologically invariant (Sec. IV-D). We then derive analogue conditions for grey-level (Sec. IV-E) and label images (Sec. IV-F).

A. Preliminary remarks

We consider the Eulerian transformation model (Sec. II-B), and we first focus on binary images. In other words, given an image $I \in \mathcal{IM}_{\mathbb{B}}$ and a discrete rigid transformation $T \in \mathcal{RIG}_{\mathbb{Z}^2}$ (intrinsically associated to a rigid transformation $\mathcal{T} \in \mathcal{RIG}_{\mathbb{R}^2}$), we consider the transformed image $I_T \in \mathcal{IM}_{\mathbb{B}}$ defined as

$$I_T = I \circ T = I \circ \mathcal{D} \circ \mathcal{T}_{|\mathbb{Z}^2} \quad (11)$$

By setting $\Omega = I^{-1}(\{1\})$, $\overline{\Omega} = I^{-1}(\{0\})$, $\Omega_T = I_T^{-1}(\{1\})$, and $\overline{\Omega_T} = I_T^{-1}(\{0\})$, Eq. (11) rewrites as

$$\Omega_T = \mathbb{Z}^2 \cap \mathcal{T}^{-1}(\Omega \oplus \square) \quad (12)$$
$$\overline{\Omega_T} = \mathbb{Z}^2 \cap \mathcal{T}^{-1}(\overline{\Omega} \oplus \square) \quad (13)$$

where $\oplus$ is the dilation operator defined in mathematical morphology [38, Ch. 1], and $\square \subset \mathbb{R}^2$ is the unit square, namely a pixel. These equations can lead to different results depending on the definition of this pixel, *i.e.*, whether $\square = [-\frac{1}{2}, \frac{1}{2}]^2$ or $]-\frac{1}{2}, \frac{1}{2}[^2$. This motivates the next remark.

Remark 8: We assume that $\mathcal{T}$ and T are such that $\mathbb{Z}^2$ does not intersect any transformed pixel border. In other words, we consider that Eqs. (11)–(13) lead to identical results for both (open or closed) definitions of $\square$. From a theoretical viewpoint, this allows us to develop a general discussion without confusing variants related to $\mathcal{D}$. From a practical viewpoint, this assumption is compliant with computer-based applications, that generally rely on floating point arithmetic.

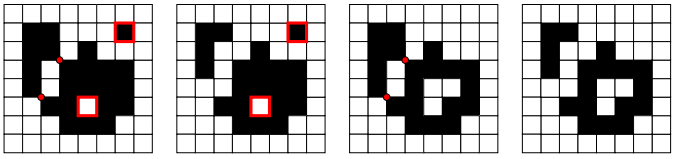

(a) (b) (c) (d)

Fig. 3. Examples of images being (a) singular and ill-composed, (b) singular and well-composed, (c) neither singular nor well-composed, and (d) not singular but well-composed. Red dots identify ill-composedness, while red boundaries identify singularity.

B. Image space restrictions

We first state that the binary images considered for the study of topological invariance can be chosen in a subspace of $\mathcal{IM}_{\mathbb{B}}$.

Remark 9: We restrict our study of $(k,\overline{k})$-topological invariance within the binary images, to the subspace $\mathcal{WC}_{\mathbb{B}} \subset \mathcal{IM}_{\mathbb{B}}$. This restriction is motivated[1] by the fact that any $I \in \mathcal{IM}_{\mathbb{B}} \setminus \mathcal{WC}_{\mathbb{B}}$ presents configurations (Th. 23, in Sec.V-A) that may be non-compliant with the definition of $(k,\overline{k})$-topological invariance.

We now introduce a notion of *singularity*, and we establish that *singular* images cannot be topologically invariant, thus reducing the image subspace to consider.

Definition 10 ((Non-)singular image): Let $I \in \mathcal{IM}_{\mathbb{B}}$. We say that I is a *singular* image if

$$\exists \mathbf{p} \in \mathbb{Z}^2, \forall \mathbf{q} \in \mathbb{Z}^2, \left(\mathbf{q} \frown_4 \mathbf{p}\right) \Longrightarrow \left(I(\mathbf{p}) \neq I(\mathbf{q})\right) \quad (14)$$

otherwise I is non-singular. We note $\mathcal{NS}_{\mathbb{B}}$ the set of the well-composed images that are non-singular.

Examples of (non-)singular images are given in Fig. 3. The non-topological invariance of singular images is derived from the non-surjectivity of some rigid transformations of $\mathcal{RIG}_{\mathbb{Z}^2}$ [19], [20]. Indeed some such transforms may remove connected components composed of exactly one pixel. More precisely, we have the following proposition.

Proposition 11:

$$\mathcal{INV}_{\mathbb{B}}^{wc} \subseteq \left(\mathcal{INV}_{\mathbb{B}}^{(k,\overline{k})} \cap \mathcal{WC}_{\mathbb{B}}\right) \subseteq \mathcal{NS}_{\mathbb{B}} \quad (15)$$

The study of topological invariance is then carried out within the set of well-composed non-singular images, independently from the considered (dual adjacency or well-composedness) model.

C. Regularity

Let us now introduce a new notion that strengthens the notion of well-composedness.

Definition 12 (Regularity): Let $I \in \mathcal{NS}_{\mathbb{B}}$. Let $v \in \{0,1\}$. We say that I is *v-regular* if for any $\mathbf{p}, \mathbf{q} \in I^{-1}(\{v\})$, we have

$$\left(\mathbf{p} \frown_4 \mathbf{q}\right) \Longrightarrow \left(\exists \boxplus \subseteq I^{-1}(\{v\}), \mathbf{p}, \mathbf{q} \in \boxplus\right) \quad (16)$$

where $\boxplus = \{x, x+1\} \times \{y, y+1\}$, for $(x,y) \in \mathbb{Z}^2$. We say that I is *regular* if it is both 0- and 1-regular. We note $\mathcal{REG}_{\mathbb{B}}^1$

[1]This restriction, presented here as an arbitrary choice when considering a global topological invariant, could be thoroughly justified in the case of a local invariant. However, as discussed in Sec. III, such a proof is beyond the scope of this article.

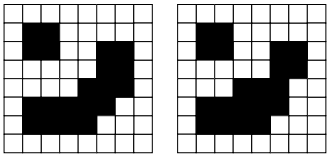

(a) (b)

Fig. 4. (a) A regular image. (b) An image that is neither 1- nor 0-regular, but that is however opened by a structuring element $\boxplus$, both for black and white points (see Rem. 13).

(resp. $\mathcal{RES}^0_{\mathbb{B}}$, resp. $\mathcal{RES}_{\mathbb{B}}$) the set of all the 1-regular (resp. 0-regular, resp. regular) binary images.

An example of a regular binary image is given in Fig. 4(a).

Remark 13: Following mathematical morphology terminology [38, Ch. 1], if I is 1- (resp. 0-) regular, then $\Omega = I^{-1}(\{1\})$ (resp. $I^{-1}(\{0\})$) is opened by any structuring element $\boxplus$, *i.e.*

$$\gamma_{\boxplus}(\Omega) = \Omega \ominus \boxplus \oplus \boxplus = \Omega \tag{17}$$

The converse is not true, as illustrated in Fig. 4(b).

D. Topological invariance: the binary case

We now establish our main theoretical result, that states that regularity implies topological invariance, for binary images.

Theorem 14:

$$\mathcal{RES}^0_{\mathbb{B}} \subseteq \mathcal{INV}^{(8,4)}_{\mathbb{B}} \tag{18}$$

$$\mathcal{RES}^1_{\mathbb{B}} \subseteq \mathcal{INV}^{(4,8)}_{\mathbb{B}} \tag{19}$$

$$\mathcal{RES}_{\mathbb{B}} \subseteq \mathcal{INV}^{wc}_{\mathbb{B}} \tag{20}$$

In the remainder of this section, this theorem (proved in App. A) is extended to grey-level and label images.

E. Topological invariance: the grey-level case

A finite grey-level image takes its values in a finite, totally ordered subset of $\mathbb{Z}$ or $\mathbb{R}$. It is then isomorphic to an image $I : \mathbb{Z}^2 \to \mathbb{G}$, where $\mathbb{G} = [\![0, m]\!] \subset \mathbb{Z}$ and $b = 0$. Without loss of generality, we then focus on such images.

A grey-level image $I \in \mathcal{IM}_{\mathbb{G}}$ is modeled by the finite set of its binary level set images $\lambda_v(I) \in \mathcal{IM}_{\mathbb{B}}$ defined, for any $v \in \mathbb{G}$ as

$$\left| \begin{array}{rcccl} \lambda_v(I) & : & \mathbb{Z}^2 & \to & \mathbb{B} \\ & & \mathbf{p} & \mapsto & \left\{ \begin{array}{ll} 1 & \text{if } v \leqslant I(\mathbf{p}) \\ 0 & \text{otherwise} \end{array} \right. \end{array} \right. \tag{21}$$

The image I can then be reconstructed as the supremum of these level set images, with respect to the pointwise order $\leq$ on functions induced by the order $\leqslant$ on $\mathbb{G}$, *i.e.*

$$I = \bigvee_{v \in \mathbb{V}}^{\leq} v.\lambda_v(I) \tag{22}$$

Based on this modelling of $I \in \mathcal{IM}_{\mathbb{G}}$ by $\{\lambda_v(I)\}_{v \in \mathbb{G}}$, the notions previously introduced for binary images can be extended to grey-levels[2] as follows

$$\mathcal{WC}_{\mathbb{G}} = \left\{ I \in \mathcal{IM}_{\mathbb{G}} \mid \forall v \in \mathbb{G}, \lambda_v(I) \in \mathcal{WC}_{\mathbb{B}} \right\} \tag{23}$$

$$\mathcal{NS}_{\mathbb{G}} = \left\{ I \in \mathcal{WC}_{\mathbb{G}} \mid \forall v \in \mathbb{G}, \lambda_v(I) \in \mathcal{NS}_{\mathbb{B}} \right\} \tag{24}$$

[2]A notion of grey-level well-composedness has also been proposed in [39].

Moreover, we can define the analogues of the binary notions of topological invariance (Def. 7) and regularity (Def. 12).

Definition 15 (Grey-level topological invariance): Let $I \in \mathcal{NS}_{\mathbb{G}}$. We say that I is $(k, \overline{k})$- (resp. wc-) *topologically invariant* if for any $v \in \mathbb{G}$, $\lambda_v(I) \in \mathcal{INV}^{(k,\overline{k})}_{\mathbb{B}}$ (resp. $\mathcal{INV}^{wc}_{\mathbb{B}}$). We note $\mathcal{INV}^{(k,\overline{k})}_{\mathbb{G}}$ (resp. $\mathcal{INV}^{wc}_{\mathbb{G}}$) the set of all the $(k, \overline{k})$- (resp. wc-) topologically invariant grey-level images.

Definition 16 (Grey-level regularity): Let $I \in \mathcal{NS}_{\mathbb{G}}$. We say that I is 1-*regular* (resp. 0-*regular*, resp. *regular*) if for any $v \in \mathbb{G}$, $\lambda_v(I) \in \mathcal{RES}^1_{\mathbb{B}}$ (resp. $\mathcal{RES}^0_{\mathbb{B}}$, resp. $\mathcal{RES}_{\mathbb{B}}$). We note $\mathcal{RES}^1_{\mathbb{G}}$ (resp. $\mathcal{RES}^0_{\mathbb{G}}$, resp. $\mathcal{RES}_{\mathbb{G}}$) the set of all the 1-regular (resp. 0-regular, resp. regular) grey-level images.

The following theorem, that is the grey-level analogue of Th. 14, straightforwardly derives from this last theorem, and Defs. 15, 16.

Theorem 17:

$$\mathcal{RES}^0_{\mathbb{G}} \subseteq \mathcal{INV}^{(8,4)}_{\mathbb{G}} \tag{25}$$

$$\mathcal{RES}^1_{\mathbb{G}} \subseteq \mathcal{INV}^{(4,8)}_{\mathbb{G}} \tag{26}$$

$$\mathcal{RES}_{\mathbb{G}} \subseteq \mathcal{INV}^{wc}_{\mathbb{G}} \tag{27}$$

Remark 18: The topological invariance (and thus, the regularity) of $I \in \mathcal{IM}_{\mathbb{G}}$ also leads to the preservation of the hierarchy of its connected components between successive levels. More precisely, the $(k, \overline{k})$- (resp. wc-) topological invariance implies that for any $T \in \mathcal{RIG}_{\mathbb{Z}^2}$, the images I and $I \circ T$ have isomorphic component-trees [40], [41], [38, Ch. 7]. This assertion is easy to prove, based on the fact that (i) T establishes a bijection between the connected components of the initial and transformed level set images (Lem. 36, in App. A), and (ii) T preserves, by construction (Eqs. (3), (21), (22)), the inclusion relation between these components at successive levels.

F. Topological invariance: the label case

A finite label image $I : \mathbb{Z}^2 \to \mathbb{L}$ is such that $\mathbb{L}$ is finite and $b \in \mathbb{L}$. Several topological frameworks have been proposed for label images [42], [43], [10], [44]. We follow a recent and general proposal [45], [46], that consists of considering the values of $\mathbb{L}$ as proto-labels, and any subsets of such values as the labels of the image. This leads to the following notions.

A label image $I \in \mathcal{IM}_{\mathbb{L}}$ is modeled by the finite set of its binary characteristic images $\chi_\Lambda(I) \in \mathcal{IM}_{\mathbb{B}}$ defined, for any $\Lambda \in 2^{\mathbb{L}}$ as

$$\left| \begin{array}{rcccl} \chi_\Lambda(I) & : & \mathbb{Z}^2 & \to & \mathbb{B} \\ & & \mathbf{p} & \mapsto & \left\{ \begin{array}{ll} 1 & \text{if } I(\mathbf{p}) \in \Lambda \\ 0 & \text{otherwise} \end{array} \right. \end{array} \right. \tag{28}$$

In particular, by identifying (i) the sets $\{l\}_{l \in \mathbb{L}}$ and $\{\{l\}\}_{l \in \mathbb{L}}$, and (ii) the monoids $(\{0,1\}, .)$ and $(\{\mathbb{L}, \emptyset\}, \cup)$, the image I can be reconstructed as the infimum of these characteristic images, with respect to the pointwise order $\sqsubseteq$ on functions induced by the inclusion order $\subseteq$ on $2^{\mathbb{L}}$, *i.e.*

$$I = \bigwedge_{\Lambda \in 2^{\mathbb{L}}}^{\sqsubseteq} \Lambda.\chi_\Lambda(I) \tag{29}$$

Based on this modelling of $I \in \mathcal{IM}_{\mathbb{L}}$ by $\{\chi_\Lambda(I)\}_{\Lambda\in 2^{\mathbb{L}}}$, the notions previously introduced for binary images can be extended[3] to label ones as follows

$$\mathcal{WC}_{\mathbb{L}} = \left\{I \in \mathcal{IM}_{\mathbb{L}} \mid \forall \Lambda \in 2^{\mathbb{L}}, \chi_\Lambda(I) \in \mathcal{WC}_{\mathbb{B}}\right\} \tag{30}$$

$$\mathcal{NS}_{\mathbb{L}} = \left\{I \in \mathcal{WC}_{\mathbb{L}} \mid \forall \Lambda \in 2^{\mathbb{L}}, \chi_\Lambda(I) \in \mathcal{NS}_{\mathbb{B}}\right\} \tag{31}$$

Moreover, we can define the analogues of the binary notions of topological invariance (Def. 7) and regularity (Def. 12).

Definition 19 (Label topological invariance): Let $I \in \mathcal{NS}_{\mathbb{L}}$. We say that I is $(k,\overline{k})$- (resp. wc-) *topologically invariant* if for any $\Lambda \in 2^{\mathbb{L}}$, $\chi_\Lambda(I) \in \mathcal{INV}_{\mathbb{B}}^{(k,\overline{k})}$ (resp. $\mathcal{INV}_{\mathbb{B}}^{wc}$). We note $\mathcal{INV}_{\mathbb{L}}^{(k,\overline{k})}$ (resp. $\mathcal{INV}_{\mathbb{L}}^{wc}$) the set of all the $(k,\overline{k})$- (resp. wc-) topologically invariant label images.

Remark 20: In the sequel, we restrict[4] our study to the case of wc-topological invariance for label images.

Definition 21 (Label regularity): Let $I \in \mathcal{NS}_{\mathbb{L}}$. We say that I is *regular* if for any $\Lambda \in 2^{\mathbb{L}}$, $\chi_\Lambda(I) \in \mathcal{RES}_{\mathbb{B}}$. We note $\mathcal{RES}_{\mathbb{L}}$ the set of all the regular label images.

The following theorem, that is the label analogue of Th. 14, straightforwardly derives from this last theorem, and Defs. 19, 21.

Theorem 22:

$$\mathcal{RES}_{\mathbb{L}} \subseteq \mathcal{INV}_{\mathbb{L}}^{wc} \tag{32}$$

V. Methodology

We have established how to guarantee topological invariance, from regularity. We now propose some algorithms to characterise regularity (Sec. V-A). Then, we describe some preprocessing strategies to turn a non-regular image into a regular, and thus a topologically invariant one (Sec. V-B).

A. Pattern-based characterisation of regular images

Regularity can be determined by considering a small set of specific patterns. This result leads to an algorithm with optimal time and space complexity.

1) Well-composedness characterisation: Regular images are necessarily well-composed. A prerequisite is then to characterise $\mathcal{WC}_{\mathbb{B}}$. This is tractable by considering a specific 2×2 pattern [29].

Theorem 23 ([29]): Let $I \in \mathcal{IM}_{\mathbb{B}}$. We have $I \notin \mathcal{WC}_{\mathbb{B}}$ iff there exist distinct points $\mathbf{p},\mathbf{q},\mathbf{r},\mathbf{s} \in \mathbb{Z}^2$, with $\mathbf{p} \frown_4 \mathbf{q} \frown_4 \mathbf{r} \frown_4 \mathbf{s} \frown_4 \mathbf{p}$, that verify

$$I(\mathbf{p}) \neq I(\mathbf{q}) \neq I(\mathbf{r}) \neq I(\mathbf{s}) \tag{33}$$

Based on Th. 23 and Defs. 15, 19, we straightforwardly derive characterisations of grey-level and label well-composedness.

Corollary 24: Let $I \in \mathcal{IM}_{\mathbb{G}}$. We have $I \notin \mathcal{WC}_{\mathbb{G}}$ iff there exist distinct points $\mathbf{p},\mathbf{q},\mathbf{r},\mathbf{s} \in \mathbb{Z}^2$, with $\mathbf{p} \frown_4 \mathbf{q} \frown_4 \mathbf{r} \frown_4 \mathbf{s} \frown_4 \mathbf{p}$, that verify

$$I(\mathbf{p}) > I(\mathbf{q}) < I(\mathbf{r}) > I(\mathbf{s}) < I(\mathbf{p}) \tag{34}$$

[3]The proposed definition of well-composedness for label images is more restrictive than the one introduced in [42], that only requires that $\chi_{\{l\}}(I) \in \mathcal{WC}_{\mathbb{B}}$ for any proto-label $l \in \mathbb{L}$.

[4]As in Rem. 9 and the associated footnote, this restriction is motivated by the fact that the $(8,4)$- and $(4,8)$-topological invariance (that are equal, from there very definitions) may be proved to be equal to the wc-topological invariance. The proof of this assertion is beyond the scope of this article.

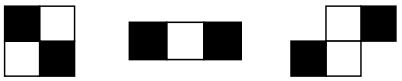

(a) (b) (c)

Fig. 5. Forbidden patterns in $\mathcal{WC}_{\mathbb{B}}$ (a) and in $\mathcal{RES}_{\mathbb{B}}^0$ (a–c), up to $\pi/2$ rotations and symmetries. The patterns forbidden in $\mathcal{RES}_{\mathbb{B}}^1$ are obtained from (a–c) by value inversion. Black (resp. white) points have value 1 (resp. 0).

Corollary 25: Let $I \in \mathcal{IM}_{\mathbb{L}}$. We have $I \notin \mathcal{WC}_{\mathbb{L}}$ iff there exist distinct points $\mathbf{p},\mathbf{q},\mathbf{r},\mathbf{s} \in \mathbb{Z}^2$, with $\mathbf{p} \frown_4 \mathbf{q} \frown_4 \mathbf{r} \frown_4 \mathbf{s} \frown_4 \mathbf{p}$, that verify

$$I(\mathbf{p}) \neq I(\mathbf{q}) \neq I(\mathbf{r}) \neq I(\mathbf{s}) \neq I(\mathbf{p}) \tag{35}$$

The characterisation of binary, grey-level and label images as well-composed can then be carried out by simply checking that they do not contain the forbidden patterns induced by Fig. 5(a).

2) Regularity characterisation: We now propose a pattern-based characterisation of regular binary images.

Proposition 26: Let $I \in \mathcal{WC}_{\mathbb{B}}$. We have $I \notin \mathcal{RES}_{\mathbb{B}}^1$ (resp. $\mathcal{RES}_{\mathbb{B}}^0$) – and *a fortiori* $\mathcal{RES}_{\mathbb{B}}$ – iff there exists $\mathbf{p} \in I^{-1}(\{1\})$ (resp. $I^{-1}(\{0\})$) that satisfies at least one of the following two conditions (up to $\pi/2$ rotations and symmetries)

$$I(\mathbf{p}-(1,0)) \neq I(\mathbf{p}) \neq I(\mathbf{p}+(1,0)) \tag{36}$$

$$I(\mathbf{p}+(0,1)) = I(\mathbf{p}) \neq I(\mathbf{p}-(1,0)) = I(\mathbf{p}+(1,1)) \tag{37}$$

Indeed, Eq. (36) is a rewriting of $I \notin \mathcal{NS}_{\mathbb{B}}$, while Eq. (37) is a rewriting of the negation of Eq. (16).

Based on Prop. 26 and Defs. 15, 19, we straightforwardly derive characterisations of grey-level and label regularity.

Corollary 27: Let $I \in \mathcal{WC}_{\mathbb{G}}$. We have $I \notin \mathcal{RES}_{\mathbb{G}}^1$ (resp. $\mathcal{RES}_{\mathbb{G}}^0$) – and *a fortiori* $\mathcal{RES}_{\mathbb{G}}$ – iff there exists $\mathbf{p} \in \mathbb{Z}^2$ that satisfies at least one of the following two conditions (up to $\pi/2$ rotations and symmetries)

$$I(\mathbf{p}-(1,0)) < I(\mathbf{p}) > I(\mathbf{p}+(1,0)) \tag{38}$$

$$\text{(resp. } I(\mathbf{p}-(1,0)) > I(\mathbf{p}) < I(\mathbf{p}+(1,0))\text{)}$$

$$I(\mathbf{p}+(0,1)) \geqslant I(\mathbf{p}) > I(\mathbf{p}-(1,0)) \geqslant I(\mathbf{p}+(1,1)) \tag{39}$$

$$\text{(resp. } I(\mathbf{p}+(0,1)) \leqslant I(\mathbf{p}) < I(\mathbf{p}-(1,0)) \leqslant I(\mathbf{p}+(1,1))\text{)}$$

Corollary 28: Let $I \in \mathcal{WC}_{\mathbb{L}}$. We have $I \notin \mathcal{RES}_{\mathbb{L}}$ iff there exists $\mathbf{p} \in \mathbb{Z}$ that satisfies at least one of the following two conditions (up to $\pi/2$ rotations and symmetries)

$$I(\mathbf{p}-(1,0)) \neq I(\mathbf{p}) \neq I(\mathbf{p}+(1,0)) \tag{40}$$

$$I(\mathbf{p}) \neq I(\mathbf{p}-(1,0)) \neq I(\mathbf{p}+(0,1)) \neq I(\mathbf{p}+(1,1)) \neq I(\mathbf{p}) \tag{41}$$

The characterisation of regular binary, grey-level and label images can then be carried out by simply checking that they do not contain the forbidden patterns induced by Fig. 5.

3) Complexity: The following result straightforwardly derives from Th. 23, Prop. 26, and their respective corollaries.

Proposition 29: Let $I \in \mathcal{WC}_{\mathbb{V}}$ (with $\mathbb{V} = \mathbb{B}$, $\mathbb{G}$ or $\mathbb{L}$). Let $\mathbb{S} \subset \mathbb{Z}^2$ such that $I^{-1}(\mathbb{V}\setminus\{b\}) \subseteq \mathbb{S}$. Characterising the regularity of I has a time complexity $\mathcal{O}(|\mathbb{S}|)$, and a space complexity $\mathcal{O}(1)$.

B. Image regularisation

We now propose two strategies for preprocessing images in order to obtain regular – and thus topologically invariant – versions, before further rigid transformation. Such strategies (i) must preserve the topological properties of the images, and (ii) should preserve as much as possible their geometric properties.

1) Iterative homotopic regularisation: A first strategy consists of locally modifying the image to eliminate the forbidden configurations defined in Eqs. (33)–(41) and Fig. 5.

Let $I \in \mathcal{IM}_{\mathbb{V}}$ (or $\mathcal{WC}_{\mathbb{V}}$, if we aim to obtain regularity, and not only 1- or 0-regularity). The problem can be expressed as a constrained optimisation one, described by

$$R(I) = \arg \min_{\mathcal{RES}^{\star}_{\mathbb{V}}(I)} D_I \tag{42}$$

where $R(I)$ is the regularised version of I; $\mathcal{RES}^{\star}_{\mathbb{V}}(I)$ is the subset of $\mathcal{RES}^{\star}_{\mathbb{V}} \in \{\mathcal{RES}^{k}_{\mathbb{V}}, \mathcal{RES}^{\overline{k}}_{\mathbb{V}}, \mathcal{RES}_{\mathbb{V}}\}$ composed by the images that have the same topology as I; and $D_I : \mathcal{IM}_{\mathbb{V}} \to \mathbb{R}_+$ is a cost function that describes a distance with respect to I, from a geometric viewpoint. (The definition of D_I actually depends on the targeted application, and can rely, *e.g.*, on Hausdorff distance, or any standard (dis)similarity measure.)

In real applications, I is defined on a finite set $\mathbb{S} \subset \mathbb{Z}^2$, and so is the space of (potential) solutions of Eq. (42). However, the size $\mathcal{O}(|\mathbb{V}|^{|\mathbb{S}|})$ of this space is huge. Then, one has to settle for an approximate solution of Eq. (42). In this context, a tractable strategy is to consider the homotopy-guided approach initially developed for monotonic transformations [47], and then adapted to non-monotonic ones [48], [49], [11], [44].

This strategy starts from the image I, and iteratively eliminates forbidden configurations by modifying the value of one point $\mathbf{p} \in \mathbb{S}$ at each iteration, until stability. This value modification can be interpreted either as a background-to-foreground or a foreground-to-background sweep, when interpreting $\mathbb{G}$ or $\mathbb{L}$ in terms of binary slice decomposition. The choice of $\mathbf{p}$ is guided (i) by D_I, *e.g.*, by following a gradient descent approach, and (ii) by choosing $\mathbf{p}$ as a simple point. This is feasible for $\mathbb{V} = \mathbb{B}$, $\mathbb{G}$ or $\mathbb{L}$ since notions of simple points have been proposed in binary [50], grey-level [51], [52] and label cases [45].

The obtained algorithm can be seen as an extension of those presented in [37], [53] for well-composedness recovery, to the case of regularity recovery. In particular, it presents the same strengths and weaknesses. Indeed, in most application cases, it will converge in linear time with respect to the number of forbidden configurations, that are often sparsely distributed within images. Nevertheless, in the worst cases (*e.g.*, in presence of fine textures, Fig. 8), it may not converge, or even fail. To deal with this issue, we propose an alternative up-sampling regularisation strategy.

2) Up-sampling regularisation: Let $I \in \mathcal{IM}_{\mathbb{V}}$ (with $\mathbb{V} = \mathbb{B}$ or $\mathbb{G}$) be a $(k, \overline{k})$-image. Even before the issue of regularisation, it may happen that I cannot be modified into a topologically-equivalent well-composed image, when using a strategy such as presented above. It is then possible to oversample I by explicitly representing its interpixel topological structure. This can be done by embedding I into the Khalimsky space [24], then leading to a new image $I_K^{(k,\overline{k})}$ defined as

$$\left| \begin{array}{rcl} I_K^{(4,8)} \; : \; \mathbb{Z}^2 & \to & \mathbb{V} \\ 2.\mathbf{p} & \mapsto & I(\mathbf{p}) \\ 2.\mathbf{p} + (0,1) & \mapsto & \bigvee^{\leqslant} I(\mathbf{p} + \{0\} \times \{0,1\}) \\ 2.\mathbf{p} + (1,0) & \mapsto & \bigvee^{\leqslant} I(\mathbf{p} + \{0,1\} \times \{0\}) \\ 2.\mathbf{p} + (1,1) & \mapsto & \bigvee^{\leqslant} I(\mathbf{p} + \{0,1\} \times \{0,1\}) \end{array} \right. \tag{43}$$

(The image $I_K^{(8,4)}$ is defined by substituting $\bigwedge$ to $\bigvee$ in Eq. (43).) The following result straightforwardly derives from these definitions.

Proposition 30: Let $I \in \mathcal{IM}_{\mathbb{V}}$ (with $\mathbb{V} = \mathbb{B}$ or $\mathbb{G}$). We have $I_K^{(k,\overline{k})} \in \mathcal{WC}_{\mathbb{V}}$. Moreover, $I_K^{(k,\overline{k})}$ and I have the same homotopy-type, when considered as $(k, \overline{k})$-images.

From now on, we then assume that $I \in \mathcal{WC}_{\mathbb{V}}$ (with $\mathbb{V} = \mathbb{B}$, $\mathbb{G}$ or $\mathbb{L}$). As stated before, even in this case, image I may still not be modified into a regular image when using homotopic iterative regularisation. Once again, an oversampling strategy can be alternatively proposed. This strategy no longer relies on Khalimsky space embedding, but on a 2×2 up-sampling approach. More precisely, from $I \in \mathcal{WC}_{\mathbb{V}}$, we can define a new image

$$\left| \begin{array}{rcl} I_{2\times 2} \; : \; \mathbb{Z}^2 & \to & \mathbb{V} \\ \mathbf{p} = (x,y) & \mapsto & I((\lfloor x/2 \rfloor, \lfloor y/2 \rfloor)) \end{array} \right. \tag{44}$$

The following result straightforwardly derives from this definition.

Proposition 31: Let $I \in \mathcal{WC}_{\mathbb{V}}$ (with $\mathbb{V} = \mathbb{B}$, $\mathbb{G}$ or $\mathbb{L}$). We have $I_{2\times 2} \in \mathcal{RES}_{\mathbb{V}}$. Moreover, $I_{2\times 2}$ and I have the same homotopy-type when considered as $(k, \overline{k})$- (resp. wc-) images.

Finally, Eqs. (43)–(44) provide a global up-sampling strategy that enables to re-cast any $(8,4)$-, $(4,8)$-, or wc-image as regular, and thus topologically invariant. This strategy has the advantages of being deterministic and geometrically preserving (up to the thickening of the interpixel space). Its main drawback, in comparison to the first strategy, is its higher spatial cost, as it models an image of size $|\mathbb{S}|$ as a new one of size $4.|\mathbb{S}|$ (and $16.|\mathbb{S}|$ in the worst cases). This may remain however acceptable for many applications, considering the memory specifications and progress of current computers.

VI. Experiments and results

In this section, we first describe experiments carried out on synthetic images (Sec. VI-A), that allow us to evaluate the behaviour of the different analysis and preprocessing strategies proposed in Sec. V. We then provide some results on real grey-level and label images (Sec. VI-B).

A. Synthetic images

1) Regularity characterisation: The regularity characterisation described in Sec. V-A, consists of looking for specific patterns that are likely to forbid the topology preservation of images during a rigid transformation. Let us consider the four binary images depicted in Fig. 6(a), that are well-composed, but neither 1- nor 0-regular. The identified forbidden patterns corresponding to this default of regularity are illustrated in

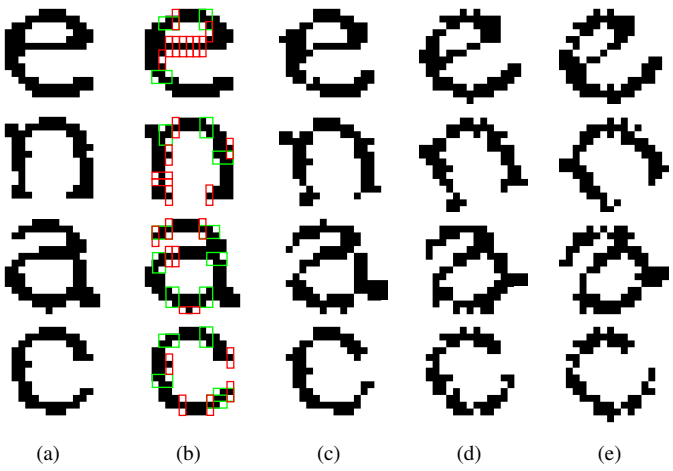

Fig. 6. (a) Four well-composed, but neither 1- nor 0-regular images. Pixels of value 1 and 0 are depicted in black and white, respectively. (b) Patterns that forbid regularity. In red: patterns of Fig. 5(b); in green: patterns of Fig. 5(c). (c–e) Three examples of rigid transformations where the four images are topologically altered in comparison to (a). In particular, the black part of the images, that are 4-connected in (a), are split into several 4-connected components. Moreover, the 8-connected components forming the holes inside the "a" and "e" letters in (a) are merged to the background.

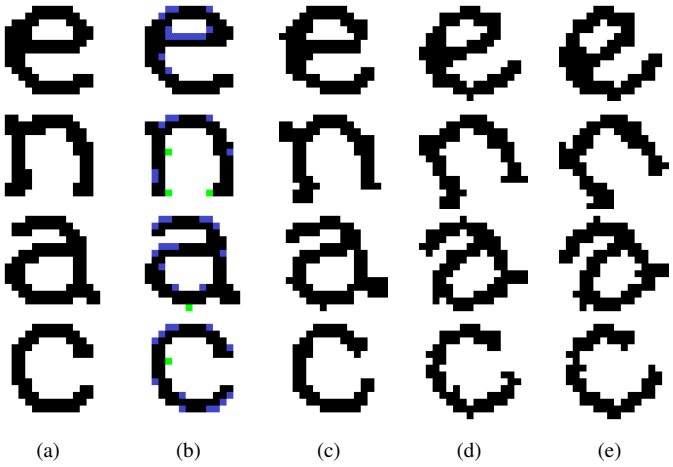

Fig. 7. (a) Regular images obtained from Fig. 6(a) after iterative homotopic regularisation. (b) Difference between (a) and Fig. 6(a). In blue: pixels switched from white to black; in green: pixels switched from black to white. (c–e) Three examples of rigid transformations where the four images are topologically preserved in comparison to (a). The transformation parameters are the same as in Fig. 6(c–e).

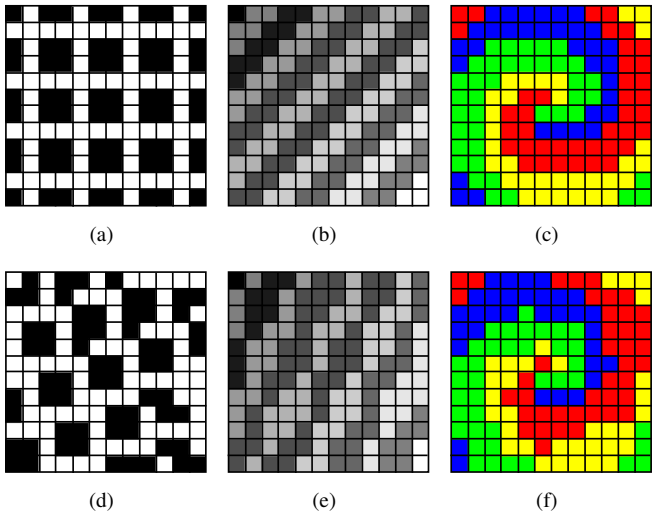

Fig. 8. (a) A well-composed binary image that is not 0-regular. Pixels of value 1 and 0 are depicted in black and white, respectively. (b) A well-composed grey-level image that is neither 1- nor 0-regular. (c) A well-composed label image that is not regular. These three images cannot be regularised without up-sampling, due to fine texture effects. (d–f) Images obtained from (a–c) after rigid transformations. They are topologically altered, in comparison to (a–c).

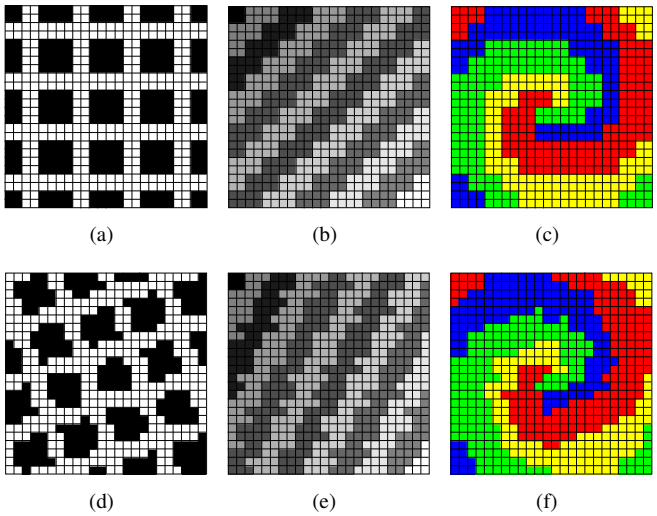

Fig. 9. (a–c) Regular images obtained from Fig. 8(a–c) after the up-sampling regularisation. (d–f) Images obtained from (a–c) after rigid transformations. They are topologically preserved, by comparison to (a–c). The transformation parameters are the same as in Fig. 8(d–f).

Fig. 6(b). Their presence indicates that the topological structure of these images is likely to be altered when applying a rigid transformation, as exemplified in Fig. 6(c–e).

2) Iterative homotopic regularisation: Let us consider the first regularisation strategy proposed in Sec. V-B, namely the iterative homotopic one. Starting from the four images of Fig. 6(a), this strategy swaps the value of simple points until a regular image with the same homotopy-type, and sufficient geometric similarity is obtained. In the results illustrated in Fig. 7(a,b), the number of modified pixels is 14, 10, 15 and 14, for each image, respectively, and the Hausdorff distance between the initial and regularised images is 1 in each case. It can be observed in Fig. 7(c–e), that for rigid transformations with the same parameters as those of Fig. 6(c–e), the obtained results now have the same topological structure as in Fig. 6(a).

3) Up-sampling regularisation: Let us now consider the three images depicted in Fig. 8(a–c), that are well-composed, but not regular, with topological consequences when applying rigid transformations, as illustrated in Fig. 8(d–f). For such images, the iterative homotopic regularisation may not converge, or even fail, due to fine texture effects. It is then relevant to consider the second, up-sampling regularisation strategy proposed in Sec. V-B.

Since the three considered images are already well-composed, it is not necessary to carry out the first step of the regularisation, namely the Khalimsky grid embedding (Eq. (43)). After the application of the second step, namely

the 2×2 up-sampling approach (Eq. (44)), we obtain new images, depicted in Fig. 9 (a–c), that are regular, and therefore topologically invariant, as illustrated in Fig. 9(d–f).

B. Real images

We now provide some regularisation results on real images.

1) Grey-level images: The first example consists of regularising the biomedical (retina) grey-level image illustrated in Fig. 10(a). This image is neither regular nor well-composed. As a consequence, a rigid transformation leads to an image that presents topological alterations, as exemplified in Fig. 10(c).

The regularisation of Fig. 10(a) aims at removing not only the configurations depicted in Fig. 5(b,c) that forbid regularity, but also those corresponding to Fig. 5(a) that more generally forbid well-composedness.

When applied on Fig. 10(a), it eliminates any configurations of Fig. 5(a–c), as illustrated in Fig. 10(b). Clearly, the regularised image is slightly modified. Indeed, due to the Khalimsky embedding, which endowes a thickness to the interpixel area, the 1-regularisation leads to an image that is dilated in a way that can be compared to the flat operations defined in mathematical morphology [38, Ch. 1]. A dual behaviour would be achieved for 0-regularisation. In particular, Fig. 10(b) is a little bit brighter than Fig. 10(a). Moreover, this image presents dimensions that are 4 times higher than those of Fig. 10(a). When applying a rigid transformation on this image, we obtain results, illustrated in Fig. 10(d), that are not topologically altered, contrarily to the transformed image of Fig. 10(c). This topological behaviour has direct consequences on the overall visual quality of the image such as its ability to be efficiently analysed. This is more easily quantifiable when considering binary images obtained by thresholding, as illustrated in Fig. 10(e–h).

2) Label images: The second example consists of regularising the label image illustrated in Fig. 11(a). This image was obtained by segmentation and clustering of multispectral remote sensing data. It is well-composed but not regular. Consequently, a rigid transformation leads to an image that presents topological alterations, as exemplified in Fig. 11(c).

When applying up-sampling regularisation on Fig. 11(a), it eliminates any configurations of Fig. 5(b–c), as illustrated in Fig. 11(b). As Fig. 11(a) is already well-composed, the first step of the regularisation, *i.e.*, the Khalimsky grid embedding, does not need to be carried out. Then, Fig. 11(b) presents dimensions that are only 2 times higher than Fig. 11(a), in contrast to the grey-level case study of Fig. 10.

When applying a rigid transformation on this regularised image, we obtain a result, illustrated in Fig. 11(d), that is not topologically altered, contrarily to the transformed image of Fig. 11(c). Such a topological behaviour is in particular desirable, *e.g.*, to analyse such images at an object-level, based on spatial reasoning [56], or to perform compositing procedures [57].

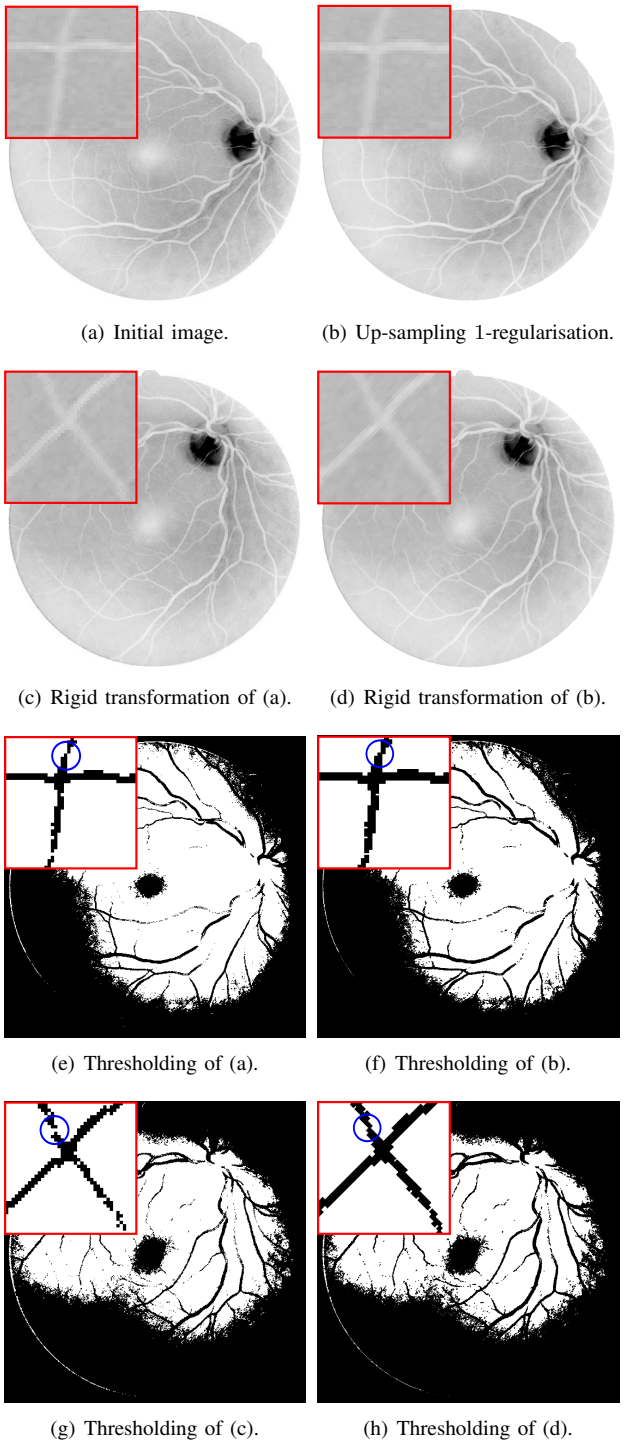

(a) Initial image. (b) Up-sampling 1-regularisation. (c) Rigid transformation of (a). (d) Rigid transformation of (b). (e) Thresholding of (a). (f) Thresholding of (b). (g) Thresholding of (c). (h) Thresholding of (d).

Fig. 10. (a) Grey-level image of dimensions 554×554 with 145 grey-levels, and a sample of dimensions 40×40 (courtesy of the DRIVE dataset [54]). It is ill-composed, and a fortiori not 1-regular. (b) 1-regular image of dimensions 2216×2216, obtained from (a) by up-sampling regularisation. (c) Image obtained from (a) by a rigid transformation. It is topologically altered, by comparison to (a). (d) Image obtained from (b) by the same rigid transformation. It is topologically preserved, by comparison to (b). (e–h) Thresholded images obtained from (a–d), respectively.

VII. Conclusion

We have investigated topology preservation of 2D digital images under rigid transformation. Based on theoretical results established in the digital topology framework, we have derived efficient algorithms for analysing and preprocessing such images. The genericity of these results and methods, in terms of topological models (dual adjacency and well-composedness)

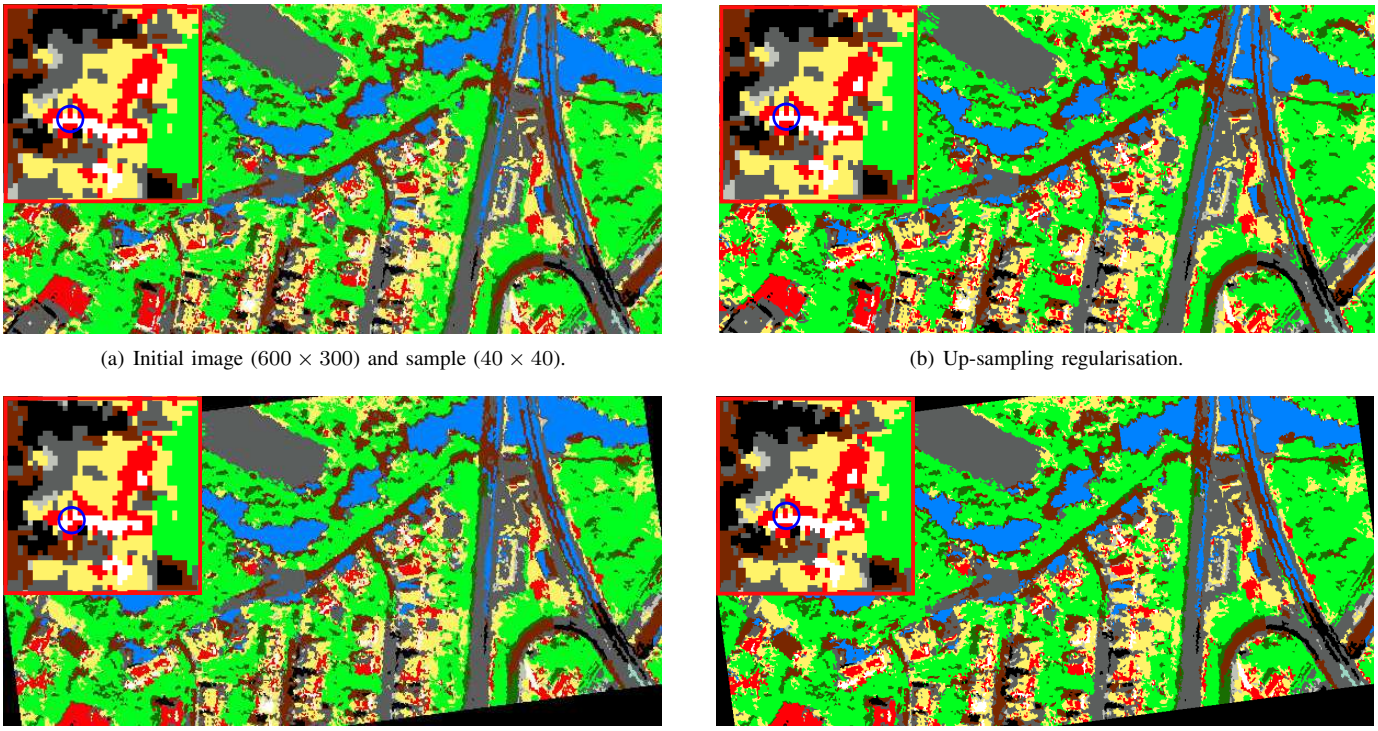

(a) Initial image (600×300) and sample (40×40).

(b) Up-sampling regularisation.

(c) Rigid transformation of (a).

(d) Rigid transformation of (b).

Fig. 11. (a) Label image of dimensions 600×300, and a sample of dimensions 40×40, segmented and clustered from a multispectral remote sensing image (courtesy Camille Kurtz [55]). This image is well-composed but not regular. (b) Regular image, of dimensions 1200×600, obtained from (a) by up-sampling regularisation. (c) Image obtained from (a) by a rigid transformation. It is topologically altered, by comparison to (a). (d) Image obtained from (b) by the same rigid transformation. It is topologically preserved, by comparison to (b).

and values (binary, grey-level and label images), authorise their actual use in real applications.

As a priority, we will seek to prove that the notion of regularity provides not only sufficient, but also *necessary* conditions for topological invariance (in other words, that the $\subseteq$ symbols in Ths. 14, 17 and 22, are indeed $=$ symbols). To this end, it will be necessary to define a relevant *local* topological invariant, relying, *e.g.*, on the topological structure that can be defined on tilings of $\mathbb{Z}^2$ induced by rigid transformations.

We will also investigate the links between our results, established in a discrete framework, and some results obtained in the research field of digitisation, that intrinsically merges both discrete and continuous frameworks. Indeed, as suggested by Eqs. (12)–(13) the rigid transformation of a digital image can be interpreted as the re-digitisation of its associated continuous pixel-based representation. Following this assertion, our notion of regularity may be seen as a discrete analogue of the notion of r-regularity developed fifteen years ago [58], [59], for topology-preserving digitisation purpose. These links are fairly intuitive but less trivial to formally establish.

From a methodological viewpoint, the next step will be to tackle $\mathbb{Z}^3$. This raises supplementary difficulties, related to the more complex definitions of topological models [60] and topological invariants [36]. To cope with this challenge, various avenues may be considered. A first possibility relies on the possible analogy between regularity and r-regularity (see above). A second way relies on a morphological interpretation of regularity. Indeed, as stated in Rem. 13, regular images are open for square structuring elements, but the converse is not true. A specific class of open images, for which the opening relies on homotopic erosions and dilations, may be considered and compared to the family of regular images, in a morpho-topological framework [61], [62], [63].

Acknowledgements

The research leading to these results has received partial funding from the French *Agence Nationale de la Recherche* (Grant Agreement ANR-10-BLAN-0205).

Appendix

A. Proof of Theorem 14

The following three properties, used in the proof of Th. 14, deal with geometric configurations already discussed in the literature (see, *e.g.*, [19]). Their easy proofs are left to the reader. (We recall that we are under the hypotheses of Rem. 8.)

Property 32: Let $\mathbf{p}, \mathbf{q} \in \mathbb{Z}^2$ such that $\mathbf{p} \frown_4 \mathbf{q}$. Let $T \in \mathcal{RIG}_{\mathbb{Z}^2}$. If $\mathbf{p} \notin T(\mathbb{Z}^2)$, then we have $\mathbf{q} \in T(\mathbb{Z}^2)$.

Property 33: Let $\mathbf{p} \in \mathbb{Z}^2$ and $T \in \mathcal{RIG}_{\mathbb{Z}^2}$ with $\mathbf{p} \notin T(\mathbb{Z}^2)$. Let $\mathbf{q}, \mathbf{r} \in \mathbb{Z}^2$ such that $\mathbf{p} \frown_4 \mathbf{q} \frown_8 \mathbf{r} \frown_4 \mathbf{p}$. There exists $\mathbf{q}', \mathbf{r}' \in \mathbb{Z}^2$ such that $T(\mathbf{q}') = \mathbf{q}$, $T(\mathbf{r}') = \mathbf{r}$, and $\mathbf{q}' \frown_4 \mathbf{r}'$.

Property 34: Let $\boxplus = \{x, x+1\} \times \{y, y+1\}$, for $(x, y) \in \mathbb{Z}^2$. We have $T^{-1}(\boxplus)/\sim_4 = \{T^{-1}(\boxplus)\}$.

The following lemma authorises the construction of the function (Eq. (45)) that will induce the isomorphism of Th. 14.

Lemma 35: Let $I \in \mathcal{RES}^1_{\mathbb{B}}$ (resp. $\mathcal{RES}^0_{\mathbb{B}}$, resp. $\mathcal{RES}_{\mathbb{B}}$). Let $T \in \mathcal{RIG}_{\mathbb{Z}^2}$. The transformation $T_{|(I \circ T)^{-1}(\{1\})}$ establishes

a homomorphism from $((I \circ T)^{-1}(\{1\}), \frown_4)$ (resp. $((I \circ T)^{-1}(\{1\}), \frown_8)$, resp. $((I \circ T)^{-1}(\{1\}), \frown_4)$) to $(I^{-1}(\{1\}), \sim_4)$ (resp. $(I^{-1}(\{1\}), \sim_8)$, resp. $(I^{-1}(\{1\}), \sim_4)$), while the transformation $T_{|(I \circ T)^{-1}(\{0\})}$ establishes a homomorphism from $((I \circ T)^{-1}(\{0\}), \frown_8)$ (resp. $((I \circ T)^{-1}(\{0\}), \frown_4)$, resp. $((I \circ T)^{-1}(\{0\}), \frown_4)$) to $(I^{-1}(\{0\}), \sim_8)$ (resp. $(I^{-1}(\{0\}), \sim_4$), resp. $(I^{-1}(\{0\}), \sim_4)$).

Proof Let $I \in \mathcal{RES}_{\mathbb{B}}$. Let $\mathbf{p}', \mathbf{q}' \in (I \circ T)^{-1}(\{1\})$ s.t. $\mathbf{p}' \frown_4 \mathbf{q}'$. Let $\mathbf{p} = T(\mathbf{p}')$, $\mathbf{q} = T(\mathbf{q}')$. We have (Eq. (11)): (i) $\mathbf{p} = \mathbf{q}$, and then $\mathbf{p} \sim_4 \mathbf{q}$; or (ii) $\mathbf{p} \frown_8 \mathbf{q}$, and then $\mathbf{p} \sim_4 \mathbf{q}$ (Def. 3). The same holds for $\mathcal{RES}_{\mathbb{B}}$ and $(I \circ T)^{-1}(\{0\})$; $\mathcal{RES}^1_{\mathbb{B}}$ and $(I \circ T)^{-1}(\{1\})$; $\mathcal{RES}^0_{\mathbb{B}}$ and $(I \circ T)^{-1}(\{0\})$. Now, let $I \in \mathcal{RES}^1_{\mathbb{B}}$. Let $\mathbf{p}', \mathbf{q}' \in (I \circ T)^{-1}(\{0\})$ s.t. $\mathbf{p}' \frown_8 \mathbf{q}'$. Let $\mathbf{p} = T(\mathbf{p}')$, $\mathbf{q} = T(\mathbf{q}')$. We have (Eq. (11)): (i) $\mathbf{p} = \mathbf{q}$, and then $\mathbf{p} \sim_8 \mathbf{q}$; (ii) $\mathbf{p} \frown_8 \mathbf{q}$, and then $\mathbf{p} \sim_8 \mathbf{q}$; or (iii) $\mathbf{p} = \mathbf{q} + (2, 0)$ or $(2, 1)$ up to $\pi/2$ rotations and symmetries, and then $\mathbf{p} \sim_8 \mathbf{q}$ (Prop. 26). The same holds for $\mathcal{RES}^0_{\mathbb{B}}$ and $(I \circ T)^{-1}(\{1\})$. ■

Let $I \in \mathcal{WC}_{\mathbb{B}}$ and $T \in \mathcal{RIG}_{\mathbb{Z}^2}$. From the above lemma, we can licitly define the function $T^\star_I$ (with $\star = (k, \overline{k})$ or wc) as

$$\left| \begin{array}{rcccl} T^\star_I & : & \mathcal{C}^\star[I \circ T] & \rightarrow & \mathcal{C}^\star[I] \\ & & C & \mapsto & T^\star_I(C) \supseteq T(C) \end{array} \right. \quad (45)$$

We are now ready to establish the first part of the isomorphism of Th. 14, namely the one-to-one mapping between the connected components of the initial and transformed images.

Lemma 36: Let $I \in \mathcal{RES}^1_{\mathbb{B}}$ (resp. $\mathcal{RES}^0_{\mathbb{B}}$, resp. $\mathcal{RES}_{\mathbb{B}}$). Let $T \in \mathcal{RIG}_{\mathbb{Z}^2}$. Then $T^{(4,8)}_I$ (resp. $T^{(8,4)}_I$, resp. T^{wc}_I) is a bijection.

Proof Let $C \in \mathcal{C}^\star[I]$. Let $\mathbf{p}, \mathbf{q} \in C$ s.t. $\mathbf{p} \frown_4 \mathbf{q}$ ($I \in \mathcal{NS}_{\mathbb{B}}$). There exists $\mathbf{p}' \in \mathbb{Z}^2$ s.t. $T(\mathbf{p}') \in \{\mathbf{p}, \mathbf{q}\} \subseteq C$ (Prop. 32). Thus, $T^\star_I$ is a surjection.

Let $I \in \mathcal{RES}_{\mathbb{B}}$. Let $C \in \mathcal{C}^\star[I]$ s.t. $C \subseteq I^{-1}(\{1\})$. For any $\mathbf{q}, \mathbf{r} \in C$, we have $(\mathbf{q} \frown_4 \mathbf{r}) \Rightarrow (\{\mathbf{q}, \mathbf{r}\} \subseteq \boxplus \subseteq C)$ (Def. 12). It follows by induction on C (Props. 33, 34) that $T^{-1}(C)/\sim_4 = \{T^{-1}(C)\}$. The same holds for $\mathcal{RES}_{\mathbb{B}}$ and $I^{-1}(\{0\})$; $\mathcal{RES}^1_{\mathbb{B}}$ and $I^{-1}(\{1\})$; $\mathcal{RES}^0_{\mathbb{B}}$ and $I^{-1}(\{0\})$. Now, let $I \in \mathcal{RES}^0_{\mathbb{B}}$. Let $C \in \mathcal{C}^\star[I]$ s.t. $C \subseteq I^{-1}(\{1\})$. For any $\mathbf{q}, \mathbf{r}, \mathbf{s} \in C$, we have $(\mathbf{q} \frown_4 \mathbf{r} \frown_4 \mathbf{s}) \Rightarrow (T^{-1}(\{\mathbf{q}, \mathbf{r}, \mathbf{s}\})/\sim_8 = \{T^{-1}(\{\mathbf{q}, \mathbf{r}, \mathbf{s}\})\})$ (Eq. (11), Props. 32, 33). It follows by induction on C that $T^{-1}(C)/\sim_8 = \{T^{-1}(C)\}$. The same holds for $\mathcal{RES}^0_{\mathbb{B}}$ and $(I \circ T)^{-1}(\{1\})$. Thus, $T^\star_I$ is an injection. ■

The following proposition is a consequence of this result.

Lemma 37: Let $I \in \mathcal{RES}^1_{\mathbb{B}}$ (resp. $\mathcal{RES}^0_{\mathbb{B}}$, resp. $\mathcal{RES}_{\mathbb{B}}$). Let $T \in \mathcal{RIG}_{\mathbb{Z}^2}$. We have $I \circ T \in \mathcal{IM}_{\mathbb{B}}$ (resp. $\mathcal{IM}_{\mathbb{B}}$, resp. $\mathcal{WC}_{\mathbb{B}}$) and $T^\star_I(B^\star_{I \circ T}) = B^\star_I$ (see Def. 6).

Proof The bijectivity of $T^\star_I$ and the fact that for any $\mathbf{p} \in \mathbb{Z}^2$, $T^{-1}(\{\mathbf{p}\})$ is finite, imply that $I \circ T \in \mathcal{IM}_{\mathbb{B}}$. We have $T^\star_I(B^\star_{I \circ T}) = B^\star_I$ for the very same reasons.

Let $I \in \mathcal{RES}_{\mathbb{B}}$. Let us suppose that $I \circ T \notin \mathcal{WC}_{\mathbb{B}}$. Then there exist distinct points $\mathbf{n}, \mathbf{e}, \mathbf{s}, \mathbf{w} \in \mathbb{Z}^2$ s.t. $\mathbf{n} \frown_4 \mathbf{e} \frown_4 \mathbf{s} \frown_4 \mathbf{w} \frown_4 \mathbf{n}$, that verify Eq. (33). From Eq. (11), we then derive that there exist distinct points $\mathbf{n}', \mathbf{e}', \mathbf{s}', \mathbf{w}' \in \mathbb{Z}^2$ s.t. $T(\mathbf{n}) = \mathbf{n}'$, $T(\mathbf{e}) = \mathbf{e}'$, $T(\mathbf{s}) = \mathbf{s}'$, $T(\mathbf{w}) = \mathbf{w}'$; moreover $\mathbf{n}' \frown_8 \mathbf{e}' \frown_8 \mathbf{s}' \frown_8 \mathbf{w}' \frown_8 \mathbf{n}'$. This authorises only three configurations, up to $\pi/2$ rotations and symmetries: (i) $\mathbf{e}' = \mathbf{n}' + (1, 0)$, $\mathbf{s}' = \mathbf{n}' + (2, -1)$, $\mathbf{w}' = \mathbf{n}' + (1, -1)$; (ii) $\mathbf{e}' = \mathbf{n}' + (1, 0)$, $\mathbf{s}' = \mathbf{n}' + (1, -1)$, $\mathbf{w}' = \mathbf{n}' + (0, -1)$; (iii) $\mathbf{e}' = \mathbf{n}' + (1, -1)$, $\mathbf{s}' = \mathbf{n}' - (0, 2)$, $\mathbf{w}' = \mathbf{n}' - (1, 1)$. But (i) corresponds to Eq. (37); (ii) to Eq. (33); and (iii) to Eq. (36); and $I \notin \mathcal{RES}_{\mathbb{B}}$: contradiction. Then we have $I \circ T \in \mathcal{WC}_{\mathbb{B}}$. ■

We are now ready to establish the last part of the isomorphism, namely the preservation of the adjacency relation.

Lemma 38: Let $I \in \mathcal{RES}^1_{\mathbb{B}}$ (resp. $\mathcal{RES}^0_{\mathbb{B}}$, resp. $\mathcal{RES}_{\mathbb{B}}$). Let $T \in \mathcal{RIG}_{\mathbb{Z}^2}$. Let $C_1, C_2 \in \mathcal{C}^\star[I \circ T]$ with $\star = (4, 8)$ (resp. $(8, 4)$, resp. wc). We have

$$\big(C_1 \frown^\star_{I \circ T} C_2\big) \Longleftrightarrow \big(T^\star_I(C_1) \frown^\star_I T^\star_I(C_2)\big) \quad (46)$$

Proof Up to reindexing, we set $C_1 \subseteq (I \circ T)^{-1}(\{0\})$ and $C_2 \subseteq (I \circ T)^{-1}(\{1\})$.

Let us suppose that $C_1 \frown^\star_{I \circ T} C_2$. Let $\mathbf{p}' \in C_1$ and $\mathbf{q}' \in C_2$ s.t. $\mathbf{p}' \frown_4 \mathbf{q}'$. Let $\mathbf{p} = T(\mathbf{p}') \in T^\star_I(C_1)$, $\mathbf{q} = T(\mathbf{q}') \in T^\star_I(C_2)$. We have (Eq. (11)): (i) $\mathbf{p} \frown_4 \mathbf{q}$ and then $T^\star_I(C_1) \frown^\star_I T^\star_I(C_2)$; or (ii) $\mathbf{p} \frown_8 \mathbf{q}$ and $\mathbf{p} \not\frown_4 \mathbf{q}$. In that case, let $\mathbf{r} \in \mathbb{Z}^2$ s.t. $\mathbf{p} \frown_4 \mathbf{r} \frown_4 \mathbf{q}$. We have either $\mathbf{r} \in T^\star_I(C_1)$ or $T^\star_I(C_2)$, and then $T^\star_I(C_1) \frown^\star_I T^\star_I(C_2)$.

Let us suppose that $T^\star_I(C_1) \frown^\star_I T^\star_I(C_2)$. Let $\mathbf{p} \in T^\star_I(C_1)$, $\mathbf{q} \in T^\star_I(C_2)$ s.t. $\mathbf{p} \frown_4 \mathbf{q}$. Case 1: $\mathbf{p}, \mathbf{q} \in T(\mathbb{Z}^2)$. Let $\mathbf{p}' \in C_1$ s.t. $T(\mathbf{p}') = \mathbf{p}$, and $\mathbf{q}' \in C_2$ s.t. $T(\mathbf{q}') = \mathbf{q}$. We have (Eq. (11)): (i) $\mathbf{p}' \frown_4 \mathbf{q}'$ and then $C_1 \frown^\star_I C_2$; (ii) $\mathbf{p}' \frown_8 \mathbf{q}'$ and $\mathbf{p}' \not\frown_4 \mathbf{q}'$: by setting $\mathbf{r}' \in \mathbb{Z}^2$ s.t. $\mathbf{p}' \frown_4 \mathbf{r}' \frown_4 \mathbf{q}'$, we have either $\mathbf{r}' \in C_1$ or C_2, and then $C_1 \frown^\star_I C_2$; (iii) $\mathbf{q}' = \mathbf{p}' + (2, 0)$, up to $\pi/2$ rotations: by setting $\mathbf{r}' = (\mathbf{p}' + \mathbf{q}')/2$, we have either $\mathbf{r}' \in C_1$ or C_2, and then $C_1 \frown^\star_I C_2$. Case 2: $\mathbf{p} \notin T(\mathbb{Z}^2)$, $\mathbf{q} \in T(\mathbb{Z}^2)$. Let $\mathbf{r} \in T^\star_I(C_1)$ and $\mathbf{s} \in T^\star_I(C_2)$ s.t. $\mathbf{p} \frown_4 \mathbf{r} \frown_8 \mathbf{s} \frown_4 \mathbf{p}$ ($I \in \mathcal{NS}_{\mathbb{B}}$). We have $\mathbf{r} \in T(\mathbb{Z}^2)$ and $\mathbf{s} \in T(\mathbb{Z}^2)$ (Prop. 32). Let $\mathbf{r}' \in C_1$ s.t. $T(\mathbf{r}') = \mathbf{r}$, and $\mathbf{s}' \in C_2$ s.t. $T(\mathbf{s}') = \mathbf{s}$. We have $\mathbf{r}' \frown_4 \mathbf{s}'$ (Prop. 34), and then $C_1 \frown^\star_I C_2$. No other cases are possible (Prop. 32). ■

Theorem 14 derives from the above three lemmas.

REFERENCES

[1] G. Bertrand, J.-C. Everat, and M. Couprie, "Image segmentation through operators based on topology," *J Electron Imaging*, vol. 6, pp. 395–405, 1997.

[2] P.-L. Bazin and D. L. Pham, "Topology-preserving tissue classification of magnetic resonance brain images," *IEEE T Med Imaging*, vol. 26, pp. 487–496, 2007.

[3] B. Zitová and J. Flusser, "Image registration methods: A survey," *Image Vision Comput*, vol. 21, no. 11, pp. 977–1000, 2003.

[4] A. Yilmaz, O. Javed, and M. Shah, "Object tracking: A survey," *ACM Comput Surv*, vol. 38, no. 4, pp. 1–45, 2006.

[5] D. L. Pham, P.-L. Bazin, and J. L. Prince, "Digital topology in brain imaging," *IEEE Signal Proc Mag*, vol. 27, no. 4, pp. 51–59, 2010.

[6] P. Soille and M. Pesaresi, "Advances in mathematical morphology applied to geoscience and remote sensing," *IEEE T Geosci Remote*, vol. 40, no. 9, pp. 2042–2055, 2002.

[7] C. A. Rothwell, J. L. Mundy, W. Hoffman, and V.-D. Nguyen, "Driving vision by topology," in *ISCV*, 1995, pp. 395–400.

[8] A. Rosenfeld and J. L. Pfaltz, "Sequential operations in digital picture processing," *J ACM*, vol. 13, no. 4, pp. 471–494, 1966.

[9] O. Duda, P. E. Hart, and J. H. Munson, "Graphical data processing research study and experimental investigation," Stanford Research Institute, Tech. Rep. AD650926, 1967.

[10] P.-L. Bazin, L. M. Ellingsen, and D. L. Pham, "Digital homeomorphisms in deformable registration," in *IPMI*, ser. LNCS, vol. 4584. Springer, 2007, pp. 211–222.

[11] S. Faisan, N. Passat, V. Noblet, R. Chabrier, and C. Meyer, "Topology-preserving warping of binary images according to one-to-one mappings," *IEEE T Image Process*, vol. 20, no. 8, pp. 2135–2145, 2011.

[12] V. Noblet, C. Heinrich, F. Heitz, and J.-P. Armspach, "3-D deformable image registration: A topology preservation scheme based on hierarchical deformation models and interval analysis optimization," *IEEE T Image Process*, vol. 14, no. 5, pp. 553–566, 2005.

[13] P. Ngo, Y. Kenmochi, N. Passat, and H. Talbot, "Combinatorial structure of rigid transformations in 2D digital images," *Comput Vis Image Und*, vol. 117, no. 4, pp. 393–408, 2013.

[14] J.-P. Reveillès, "Géométrie discrète, calcul en nombres entiers et algorithmique," Thèse d'État, Université Strasbourg 1, 1991.

[15] E. Andres, "The quasi-shear rotation," in *DGCI*, ser. LNCS, vol. 1176. Springer, 1996, pp. 307–314.

[16] M. S. Richman, "Understanding discrete rotations," in *ICASSP*, vol. 3, 1997, pp. 2057–2060.

[17] B. Nouvel and E. Rémila, "Incremental and transitive discrete rotations," in *IWCIA*, ser. LNCS, vol. 4040. Springer, 2006, pp. 199–213.

[18] Y. Thibault, Y. Kenmochi, and A. Sugimoto, "Computing upper and lower bounds of rotation angles from digital images," *Pattern Recogn*, vol. 42, no. 8, pp. 1708–1717, 2009.

[19] B. Nouvel and E. Rémila, "Configurations induced by discrete rotations: Periodicity and quasi-periodicity properties," *Discrete Appl Math*, vol. 147, no. 2–3, pp. 325–343, 2005.

[20] P. Ngo, Y. Kenmochi, N. Passat, and H. Talbot, "Sufficient conditions for topological invariance of 2D digital images under rigid transformations," in *DGCI*, ser. LNCS, vol. 7749. Springer, 2013, pp. 155–168.

[21] P. Ngo, N. Passat, Y. Kenmochi, and H. Talbot, "Well-composed images and rigid transformations," in *ICIP*, 2013, pp. 3035–3039.

[22] T. Y. Kong and A. Rosenfeld, "Digital topology: Introduction and survey," *Comput Vision Graph*, vol. 48, no. 3, pp. 357–393, 1989.

[23] L. Mazo, N. Passat, M. Couprie, and C. Ronse, "Digital imaging: A unified topological framework," *J Math Imaging Vis*, vol. 44, no. 1, pp. 19–37, 2012.

[24] E. Khalimsky, "Topological structures in computer science," *J Appl Math Sim*, vol. 1, no. 1, pp. 25–40, 1987.

[25] V. A. Kovalevsky, "Finite topology as applied to image analysis," *Comput Vision Graph*, vol. 46, no. 2, pp. 141–161, 1989.

[26] L. Mazo, N. Passat, M. Couprie, and C. Ronse, "Paths, homotopy and reduction in digital images," *Acta Appl Math*, vol. 113, no. 2, pp. 167–193, 2011.

[27] C. R. F. Maunder, *Algebraic Topology*. Dover, New York, 1996.

[28] A. Rosenfeld, "Digital topology," *Am Math Mon*, vol. 86, no. 8, pp. 621–630, 1979.

[29] L. J. Latecki, U. Eckhardt, and A. Rosenfeld, "Well-composed sets," *Comput Vis Image Und*, vol. 61, no. 1, pp. 70–83, 1995.

[30] T. Y. Kong, "A digital fundamental group," *Comput Graph*, vol. 13, no. 2, pp. 159–166, 1989.

[31] C. Ronse, "A topological characterization of thinning," *Theor Comput Sci*, vol. 43, no. 1, pp. 31–41, 2007.

[32] G. Bertrand and G. Malandain, "A new characterization of three-dimensional simple points," *Pattern Recogn Lett*, vol. 15, no. 2, pp. 169–175, 1994.

[33] G. Bertrand, "On P-simple points," *CR Acad Sci I-Math*, vol. I, no. 321, pp. 1077–1084, 1995.

[34] N. Passat and L. Mazo, "An introduction to simple sets," *Pattern Recogn Lett*, vol. 30, no. 15, pp. 1366–1377, 2009.

[35] A. Rosenfeld, "Adjacency in digital pictures," *Inform Control*, vol. 26, no. 1, pp. 24–33, 1974.

[36] G. Bertrand, M. Couprie, and N. Passat, "A note on 3-D simple points and simple-equivalence," *Inform Process Lett*, vol. 109, no. 13, pp. 700–704, 2009.

[37] A. Rosenfeld, T. Y. Kong, and A. Nakamura, "Topology-preserving deformations of two-valued digital pictures," *Graph Model Im Proc*, vol. 60, no. 1, pp. 24–34, 1998.

[38] L. Najman and H. Talbot, Eds., *Mathematical Morphology: From Theory to Applications*. ISTE/J. Wiley & Sons, 2010.

[39] J. Marchadier, D. Arquès, and S. Michelin, "Thinning grayscale well-composed images," *Pattern Recogn Lett*, vol. 25, no. 5, pp. 581–590, 2004.

[40] P. Salembier, A. Oliveras, and L. Garrido, "Anti-extensive connected operators for image and sequence processing," *IEEE T Image Process*, vol. 7, no. 4, pp. 555–570, 1998.

[41] P. Salembier and M. H. F. Wilkinson, "Connected operators: A review of region-based morphological image processing techniques," *IEEE Signal Proc Mag*, vol. 26, no. 6, pp. 136–157, 2009.

[42] L. J. Latecki, "Multicolor well-composed pictures," *Pattern Recogn Lett*, vol. 16, no. 4, pp. 425–431, 1995.

[43] Y. Cointepas, I. Bloch, and L. Garnero, "A cellular model for multi-objects multi-dimensional homotopic deformations," *Pattern Recogn*, vol. 34, no. 9, pp. 1785–1798, 2001.

[44] G. Damiand, A. Dupas, and J.-O. Lachaud, "Fully deformable 3D digital partition model with topological control," *Pattern Recogn Lett*, vol. 32, no. 9, pp. 1374–1383, 2011.

[45] L. Mazo, N. Passat, M. Couprie, and C. Ronse, "Topology on digital label images," *J Math Imaging Vis*, vol. 44, no. 3, pp. 254–281, 2012.

[46] L. Mazo, "A framework for label images," in *CTIC*, ser. LNCS, vol. 7309. Springer, 2012, pp. 1–12.

[47] E. R. Davies and A. P. Plummer, "Thinning algorithms: A critique and a new methodology," *Pattern Recogn*, vol. 14, no. 16, pp. 53–63, 1981.

[48] J.-F. Mangin, V. Frouin, I. Bloch, J. Régis, and J. López-Krahe, "From 3D magnetic resonance images to structural representations of the cortex topography using topology preserving deformations," *J Math Imaging Vis*, vol. 5, no. 4, pp. 297–318, 1995.

[49] X. Han, C. Xu, and J. L. Prince, "A topology preserving level set method for geometric deformable models," *IEEE T Pattern Anal*, vol. 25, no. 6, pp. 755–768, 2003.

[50] M. Couprie and G. Bertrand, "New characterizations of simple points in 2D, 3D, and 4D discrete spaces," *IEEE T Pattern Anal*, vol. 31, no. 4, pp. 637–648, 2009.

[51] M. Couprie, F. N. Bezerra, and G. Bertrand, "Topological operators for grayscale image processing," *J Electron Imaging*, vol. 10, no. 4, pp. 1003–1015, 2001.

[52] ——, "A parallel thinning algorithm for grayscale images," in *DGCI*, ser. LNCS, vol. 7749. Springer, 2013, pp. 71–82.

[53] M. Siqueira, L. J. Latecki, N. J. Tustison, J. H. Gallier, and J. C. Gee, "Topological repairing of 3D digital images," *J Math Imaging Vis*, vol. 30, no. 3, pp. 249–274, 2008.

[54] J. J. Staal, M. D. Abramoff, M. Niemeijer, M. A. Viergever, and B. van Ginneken, "Ridge based vessel segmentation in color images of the retina," *IEEE T Med Imaging*, vol. 23, no. 4, pp. 501–509, 2004.

[55] C. Kurtz, N. Passat, P. Gançarski, and A. Puissant, "Extraction of complex patterns from multiresolution remote sensing images: A hierarchical top-down methodology," *Pattern Recogn*, vol. 45, no. 2, pp. 685–706, 2012.

[56] J. Inglada and J. Michel, "Qualitative spatial reasoning for high-resolution remote sensing image analysis," *IEEE T Geosci Remote*, vol. 47, no. 2, pp. 599–612, 2009.

[57] P. Soille, "Morphological image compositing," *IEEE T Pattern Anal*, vol. 28, no. 5, pp. 673–683, 2006.

[58] A. Gross and L. Latecki, "Digitizations preserving topological and differential geometric properties," *Comput Vis Image Und*, vol. 62, no. 3, pp. 370–381, 1995.

[59] L. J. Latecki, C. Conrad, and A. Gross, "Preserving topology by a digitization process," *J Math Imaging Vis*, vol. 8, no. 2, pp. 131–159, 1998.

[60] L. J. Latecki, "3D well-composed pictures," *Comput Vision Graph*, vol. 59, no. 3, pp. 164–172, 1997.

[61] C. Ronse, "Set-theoretical algebraic approaches to connectivity in continuous or digital spaces," *J Math Imaging Vis*, vol. 8, no. 1, pp. 41–58, 1998.

[62] J. Serra, "Connectivity on complete lattices," *J Math Imaging Vis*, vol. 9, no. 3, pp. 231–251, 1998.

[63] U. Braga-Neto and J. K. Goutsias, "A theoretical tour of connectivity in image processing and analysis," *J Math Imaging Vis*, vol. 19, no. 1, pp. 5–31, 2003.

Phuc Ngo graduated from the post-secondary preparatory curriculum at the University of Science and Technology of Danang in Vietnam. She was admitted to the research-oriented curriculum in Computer Science, majoring in Image Processing and graduated from the University of Aix-Marseille, France in 2010. In 2013, she received the PhD degree in Computer Science from Paris-Est University, France. She is now a post-doc researcher at CEA, France. Her search interests include digital geometry and topology, in particular in relation to geometric transformations and tomography.

Nicolas Passat obtained the MSc and PhD from Université Strasbourg 1 in 2002 and 2005, and Habilitation from Université de Strasbourg in 2011. He was a post-doc researcher at Université Paris-Est / ESIEE-Paris, France, in 2006. He was an assistant professor at Université de Strasbourg, France, between 2006 and 2012. He is now a full professor at Université de Reims Champagne-Ardenne, France. His scientific interests include mathematical morphology, discrete topology, medical imaging and remote sensing.

Yukiko Kenmochi received her B. Eng., M. Eng., and D. Eng. degrees in information and computer sciences from Chiba University, Japan, in 1993, 1995, and 1998, respectively. She joined Japan Advanced Institute of Science and Technology as a research associate in 1998, and Okayama University, Japan, as a lecturer in 2003. Since 2004, she has been a CNRS research associate at Laboratoire d'Informatique Gaspard-Monge, Université Paris-Est, and a member of the research group A3SI. Her research interests include discrete geometry for computer imagery.

Hugues Talbot graduated from École Centrale de Paris in 1989, obtained the MSc from Université Paris 6 in 1990 and the PhD from École des Mines de Paris in 1993. He was a principal research scientist at CSIRO, Sydney, Australia, between 1994 and 2004. He is now an associate professor at Université Paris-Est / ESIEE in Paris, France. He is the co-author or co-editor of 6 books and has published over 120 articles in the area of image processing, image analysis and computer vision. He is the recipient of several prizes including the DuPont innovation award in 2006 for his work in medical imaging. His main interests include mathematical morphology, discrete geometry, combinatorial and continuous optimization.